CIRP Annals - Manufacturing Technology 58 (2009) 701–721

Contents lists available at ScienceDirect

CIRP Annals - Manufacturing Technology

journal homepage: http://ees.elsevier.com/cirp/default.asp

Multisensor data fusion in dimensional metrology

A. Weckenmann (1)[a,*], X. Jiang (2)[b], K.-D. Sommer[c], U. Neuschaefer-Rube[c], J. Seewig[d], L. Shaw[a], T. Estler (1)[e]

[a] Chair Quality Management and Manufacturing Metrology, University Erlangen-Nuremberg, Naegelsbachstrasse 25, 91052 Erlangen, Germany
[b] Centre for Precision Technologies, University of Huddersfield, UK
[c] Physikalisch-Technische Bundesanstalt, Braunschweig, Germany
[d] Institute for Measurement and Sensor Technology, University Kaiserslautern, Germany
[e] National Institute of Standards and Technology, Gaithersburg, MD, USA

ARTICLE INFO

Keywords:
Dimensional metrology
Sensor
Data fusion

ABSTRACT

Multisensor data fusion in dimensional metrology is used in order to get holistic, more accurate and reliable information about a workpiece based on several or multiple measurement values from one or more sensors. The theoretical background originates in classical mathematics and statistics, in methods of artificial intelligence (AI) and in the Bayesian fusion approach. Sensor technologies and sensor characteristics influence the data fusion process and determine the gain of information compared to the application of a single sensor. Homogeneous and inhomogeneous sensor configurations lead to complementary, competitive and cooperative information integration with specific advantages depending on the application. The scope includes image fusion, tactile and optical coordinate metrology, coherent and incoherent optical measuring techniques, computed tomography as well as scanning probe microscopes.

1. Purpose and basics of data fusion in metrology

1.1. Introduction

Since the requirements on the complexity and accuracy of dimensional metrology are increasing, multisensor data fusion methods are employed to achieve both holistic geometrical measurement information and improved reliability or reduced uncertainty of measurement data to an increasing extent. This paper reviews the process of data fusion and gives examples of its applications in dimensional metrology.

1.1.1. Definition

Multisensor data fusion in dimensional metrology can be defined as the process of combining data from several information sources (sensors) into a common representational format in order that the metrological evaluation can benefit from all available sensor information and data. This means that measurement results can be determined, which could not – or only with worse accuracy – be determined solely on the basis of data from an individual source (sensor) only.

1.1.2. Tasks and objectives

The basic motivation for multisensor data fusion is the improvement in the quality and usability of the measurement result, e.g. in a production process. Measurement of (often multivariate or complex) quantities is enabled which are not accessible with single-sensor systems. This additional metrological benefit may be termed synergy. Synergistic effects may improve the performance of a system in at least one of the following ways: increased spatial and temporal coverage and better resolution, increased robustness to sensor and algorithmic uncertainty, better noise suppression and improved accuracy [48]. Particular features of a workpiece can be measured with the most suitable sensor, and measurements with small uncertainty can be used to correct data from other sensors which exhibit relevant systematic errors but have a wider field of view or application range.

1.1.3. Characteristics of information sources

Sensors of a similar type which capture the same or a comparable physical measurand are called homogeneous sensors. An example is the use of cameras with different observation parameters. On the other hand inhomogeneous sensors acquire different characteristics of a scene. Here the information is not directly linkable and pre-processing is necessary (e.g. feature extraction, classification, data compression). An example is the fusion of greyscale images and 3D-data.

1.1.4. Sensor configuration

Multisensor fusion describes the synergistic application of different (homogenous and inhomogeneous) sensors to perform a given measuring task. The kind of integration of multiple sensors into a multisensor system depends on the application and the kind of sensor data or signal (Fig. 1).

Durrant-Whyte [46] classifies a multisensor data fusion system after its sensor configuration in the categories competitive, complementary and cooperative integration.

* Corresponding author.

0007-8506/$ – see front matter © 2009 CIRP.
doi:10.1016/j.cirp.2009.09.008

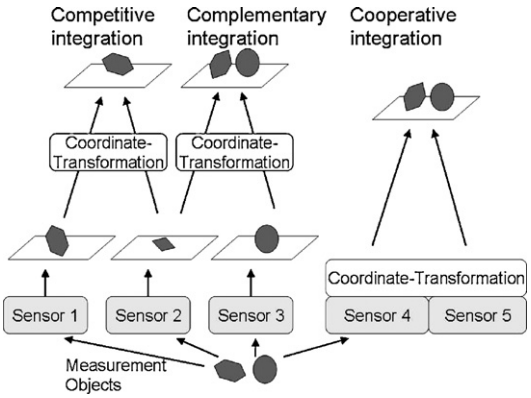

Fig. 1. Methods for data acquisition. Based on [160].

A sensor configuration is called complementary if the sensors do not directly depend on each other, but can be combined in order to give a more complete image of the phenomenom under observation. Complementary sensors help to resolve the problem of incompleteness. An example being images captured by homogeneous sensors with varying distance to the object surface showing different locations on the surface in focus according to the height of the surface. The locations, which show the highest contrast, are then fused for the final result [150]. Other examples are the fusion of images captured with different illumination series to achieve images with higher contrast [81] or the stitching of images captured by one or more moving or motionless cameras [135].

A sensor configuration is competitive if each sensor delivers an independent measurement of the same property, e.g. an image sensor captures data from the same measurement area and the redundant information is fused by evaluating the mean for each pixel. Thereby all images of the series contribute equally to the fusion result [85]. The aim of competitive fusion is to reduce the measurement uncertainty and to avoid erroneous measurements.

A cooperative sensor configuration uses the information provided by two, or more, independent (inhomogeneous) sensors to derive information that would not be available from the sensors individually. The evaluation leads to increased information of object details and an elimination of ambiguities. Often, cooperative sensor configurations allow measurands (multivariate or multidimensional) that could not previously be evaluated to be measured. A practical example would be the case of multisensor coordinate measuring machines (CMMs) integrating different high precision sensors such as optical and tactile sensors and computed tomography.

1.1.5. Data sets (point clouds)

Data sets can be classified with reference to their origin or source and, hence, with physical measurement information they represent. In dimensional measurement, relevant examples are given with

- Intensity images (e.g. from CCD cameras)
- Surface descriptions (e.g. tactile or optical sensor data)
- Volume data (e.g. computed tomography (CT)- or MR-magnetic-resonance data)

If data sets represent points on the surface of a workpiece or of a feature, they are often named "point clouds".

1.1.6. Classification in accordance with fusion aspects

Boudjemaa and Forbes [15] classify the data fusion problems according to the aspect the data is fused:

- Fusion across sensors
- Fusion across attributes
- Fusion across domains
- Fusion across time (filtering)

Fusion across sensors: A number of sensors nominally measure the same property, such as, e.g. a number of tactile and optical sensors measuring the dimension of an object obtaining two or more volume data sets.

Fusion across attributes: In this situation, a number of sensors measure different quantities associated with the same experimental situation. Consider, for example, the measurement of the length of a gauge block by a laser-interferometric system. The displacement measured by the interferometer depends on the refractive index of air which in turn depends on air temperature, pressure and humidity [14]. The length of the gauge block also depends on its own temperature which also has to be monitored. Thus, in order to determine the gauge-block length, up to five sensors are required to capture all relevant input quantities such as interferometer fringe counts, air temperature, air pressure, humidity and artefact temperature.

Fusion across domains: A number of sensors measure the same attribute over various ranges or domains. This arises for example in triangulation or photogrammetry. Another example is the fusion of two images of an object taken from different viewpoints under different illumination conditions. In such cases the desired information can only be obtained by combining a series of images, yielding a new or an enhanced representation of the image contents or characteristics [173]. Another example is the fusion of data sets of two or more range images of an object taken from different viewpoints (e.g. to overcome limitations of optical sensors on the maximum detectable slope [122,123]) or data sets of different dimensions (e.g. intensity image and range image).

Fusion across time: New measurement data are fused with historical information, which, for example, could originate from an earlier calibration. Often the current information is not sufficient to determine the system accurately and historical information has to be incorporated to achieve this. This fusion across time is realized, for example in predicting filtering in dynamic measurement (parameter estimation of dynamic systems), such as in Kalman filters. Further examples: Two range images of a moving or vibrating object taken from almost the same (relative) viewpoint but at different times or sequentially measured volume data sets of the same object measured by the same device (filtering).

Two further classifications for data fusion are

- Fusion for information gain
- Fusion for information evaluation

2. Theoretical aspects of multisensor fusion and integration

Multisensor data fusion based on different information sources involves the following operations:

- Pre-processing
- Registration
- Optimization
- Data fusion
- Data reduction (optional)
- Meshing (optional)
- Data format conversion (optional)

As first step the sensor data typically is pre-processed at the necessary level of abstraction. Afterwards the sensor data are transformed into a common coordinate system (registration) evaluating items such as features. Before the final data fusion an optimization is run, taking *a priori* knowledge into account. The optimization results in an 'instruction' of how the fusion result is to be achieved based on the measuring data and additional knowledge.

2.1. Pre-processing at fusion levels

In data fusion information can be raw data provided by multiple sensors as well as a mathematical interpretation

of their data. Different levels of abstraction are differentiated [40]:

- Signal level
- Feature level
- Symbol level

On signal level (in image registration also called pixel level) the sensor data are directly combined. Requirements are the comparability of the measurement data and their registration.

Feature level: Signal descriptors are fused to achieve better estimated values of certain signal characteristics. Fusion can be applied at the feature level, if there is no temporal or spatial coherence between the sensor data on the signal level.

Symbol level: Detection- or classification-results are combined to make a decision based on a probability density function.

Fusion on a higher level of abstraction is usually more efficient, though in the field of dimensional metrology not necessarily more effective, as data reduction is involved [159]. In dimensional metrology data fusion is usually applied at the signal level, but it can also be necessary to implement other levels of abstraction, e.g. in the case of fusing data captured with diffuse illumination (greyscale images) and data captured with laserscanners or triangulation sensors (3D maps). Here a level of abstraction is necessary which considers the reflectance and geometrical characteristics of the specimens [108].

2.2. Registration

2.2.1. Motivation and definition

Registration is one of the most important and decisive steps of multisensor data fusion. The registration process is the prior step before data fusion, during which the measurement data captured in the respective sensor's coordinate system are aligned and transformed to one common coordinate system. The transformation parameters can include three rotations and 3D lateral shift. Commonly the criterion for determining the transformation parameters is the Least Square Criterion. This involves the minimization of the variance of distances of corresponding points in the sensor data or of corresponding points in overlapping areas. When data sets (e.g. images) are acquired with different magnifications, scale adjustment may also be necessary.

The registration can be either feature based or based on surface descriptions [173]. Feature-based registration requires corresponding areas/points on the workpiece or on the supporting plate or in the vicinity. It is a very accurate alignment method if there are a sufficient number of well-conditioned features with a sufficiently small uncertainty. Significant regions, lines or points can be understood as features. They must be unique and spread uniformly over the entire data set. They are expected to be stable in time and immovable during the measurement. The features represent information on a higher level. This property makes feature-based methods suitable for situations when variations such as illumination changes are expected. The use of feature-based methods is recommended if the measurement data contain enough distinguishable and easily detectable features. It is also possible, although not in all cases, to compensate for the lack of distinctive objects by the introduction of extrinsic features (e.g. markers).

Sometimes it is desirable for the registration process to be done in two steps: coarse and fine registration. In these cases the data sets which are to be superimposed may be of different resolutions or acquired at different viewpoints or with different sensors. In such cases no additional measurement uncertainty, which is significant compared to the uncertainty of the sensor data, should be generated.

2.2.2. Methods of registration

This overview intends to cover 3D registration methods. A good overview on 2D registration methods has been previously given in [211]. The application of markers is one method to register three-dimensional data sets. Other methods use the knowledge about the sensor positions to transform the data sets into one coordinate system. A third possibility applies numerical methods, which are divided into coarse and fine registration processes. During coarse registration the first alignment of data sets is done using feature-based strategies [173,164,170]. During fine registration standard optimization techniques try to find an extremum of a given similarity metric taking the entire data set into account. The iterative closest point (ICP) algorithm needs no feature extraction and has become an important standard for fine registration of point clouds [10,61,69].

2.2.3. Coordinate transformation with uncertainty propagation

Whereas the above listed methods are based on affine transformations, there are further approaches which take the uncertainty propagation during the coordinate transformation into account. Fig. 2 illustrates this with an example of vehicle state estimation [190]: The (best estimate of the) state $\mathbf{X}_{A1}$ (position, speed, etc.) of an object #1 is determined by the tracking system of a vehicle *A* the (best estimate of the) state of which is described by the vector $\mathbf{X}_{0A}$. Hence, the best estimate of the state of the object #1 in the "global coordinate system" is given by the transformation:

$$E[\boldsymbol{X}_{01}] := E[\boldsymbol{X}_{0A}] \oplus E[\boldsymbol{X}_{A1}], \tag{1}$$

where $E[\mathbf{X}]$ is the expectation of the vector $\mathbf{X}$.

The resulting (joint) co-variance matrix associated with the above transformation result is obtained by utilizing the law of Gaussian uncertainty propagation:

$$\boldsymbol{C}_{\boldsymbol{X}01} \approx J_{\oplus} \begin{pmatrix} \boldsymbol{C}_{\boldsymbol{X}0A} & \boldsymbol{C}_{\boldsymbol{X}0A\boldsymbol{X}A1} \\ \boldsymbol{C}_{\boldsymbol{X}A1\boldsymbol{X}0A} & \boldsymbol{C}_{\boldsymbol{X}A1} \end{pmatrix} J'_{\oplus} T, \tag{2}$$

where $J_{\oplus}$ is the Jacobian Matrix (of the sensitivity coefficients) of the transformation process. The diagonal elements, $\mathbf{C}_{\mathbf{X}0A}$ and $\mathbf{C}_{\mathbf{X}A1}$, are the squared uncertainties, i.e. the variances associated with the state vectors $\mathbf{X}_{0A}$ and $\mathbf{X}_{A1}$; all other elements are co-variances. Backward transformations and loops in coordinate transformation for data/information registration are to be avoided because they would result in significantly increased uncertainties without gaining additional information.

2.3. Methods of data fusion

During the fusion process it is decided which measurement data is integrated into the final data set and how redundant data are combined. In regions containing redundant measurement data, quality criteria, such as the measurement uncertainty, have to be taken into account [145]. This can be done by estimation, inference, fuzzy or neural methods [12,1,13,36,38,56,74,75,103,104,133,183,185,190].

2.3.1. Estimation methods

Basically, useful information can be provided by any source, sensor, other data sources, *a priori* knowledge and the like. Based on the information provided by the sources and the information about the factors (parameters) influencing the measurement process, such as the environmental temperature, both a single-sensor measurement and multisensor measurements may be seen and treated as parameter estimation problem.

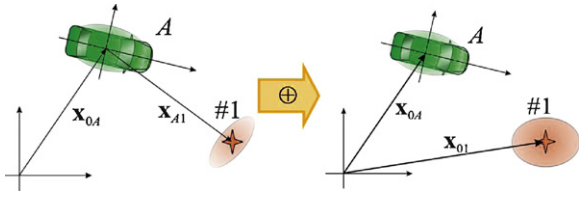

Fig. 2. Example of a coordinate transformation with uncertainty propagation [190].

Accordingly, a single-sensor measurement is a parameter estimation problem concerning both the value of a measurand Y and the uncertainty associated with it. Note that the value of the measurand is an idealization and cannot be measured directly; it is basically unknowable. The measurement process provides one or more observations q_k (values or sensor signals) that contain information both about the measurand and the measurement process. To exploit the knowledge on the measurand optimally, the measurement process ($Y \rightarrow Q$) needs to be reconstructed, taking into account the available additional information on the internal and external quantities and parameters influencing the measurement result [103].

To estimate the value of the measurand Y, a causal interrelation between Y and an assigned quantity Q is presupposed, where the measurand Y constitutes the cause, and the (sample) observations q_k of Q represent the effect, such that the observations q_k can be used to estimate Y. However, due to unavoidably incompletely known (systematic) disturbances and influences X_i and the imperfection of the measuring process (represented by the mapping $Y \rightarrow q_k$), an unambiguous computation of Y is not possible.

Fig. 3 illustrates this estimation model. A parameter source provides the parameter to be measured, i.e. the measurand Y. A measuring instrument is used to perform a measurement yielding the (sample) observations q_k, which are assumed to be realizations of the (random) variable Q.

According to Fig. 3, two different information states can be distinguished. State 1 encompasses the knowledge necessary to obtain a "first estimate" of the measurand Y based on a single observation q as well as, possibly, vague information on Y, if any. Within this information state, the estimation block is typically reduced to the application of a (usually inverse) mathematical model of the measurement to compute an estimate of Y based on a (single) observation q. State 2 additionally includes information on further (repeated) observations. The estimate of the value of Y is then usually determined in accordance with the classical statistical sampling analysis. Step 3 is the inclusion of *a priori* knowledge about both the measuring process and external influences. Additionally, *a priori* knowledge about the measurand might be incorporated.

When various measurement results obtained for the same measurand or for a regression plot are combined, Least Square Analysis and Weighted Average are appropriate estimation methods. They are typically applied to steady-state measurements [15,53]. In processing of time-dependent and time-discretised digital measurement signals, Kalman Filtering and its further developments are usually used as model-based stochastic state-estimators [26,60]. The Kalman Filter is a set of mathematical equations providing efficient computational recursive means to estimate the state of a dynamic (measurement) process by minimizing the mean of the squared error. It supports estimations of the past, the present and even future aspects. It can do so even when the precise nature of the modelled system remains unknown [195]. One may understand the Kalman Filter as an application of the Least Squares Analysis to a state estimation of time-variant quantities/variables. However, the classical Kalman Filter [101] is confined to known correlations and (time-discretised) linear (measuring) systems. Extended Kalman Filters and other analytical filters can cope with non-linear systems; however, as the classical Kalman Filter, they need to know the correlations [163]. So-called boundary densities and co-variance bound can cope with unknown correlations [76] and are, therefore, appropriate mathematical tools for uncertainty analysis and measurement data fusion of dynamic measuring systems.

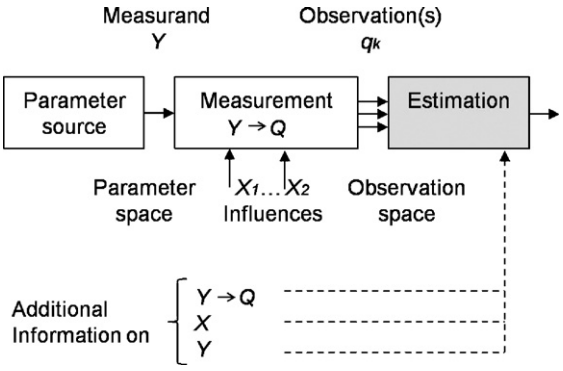

Fig. 3. Measurement as parameter estimation model.

Basically, in the time domain, a dynamic system can be described by means of ordinary differential equations or by a so-called system equation in (discretised) state-space form [106]:

$$Z_{k+1} = A_k Z_k + B_k X_{\mathrm{IN}k} \tag{3}$$

where Z_k is the so-called State Vector at an instant point of time, A_k and B_k are transition matrices containing constant factors only, and $X_{\mathrm{IN}k}$ is the vector of the input signals [107].

2.3.2. Inference methods

Modern probabilistic approaches express any kind of information in a unique and mutually compatible manner. In particular, the Bayesian probability theory utilizes probability density functions (PDF) in a degree-of-belief interpretation to express, process or combine arbitrary states of information [104]. This applies to both measurement data evaluation and contemporary uncertainty determination [94,95].

In measurement, for assigning an appropriate PDF to a certain kind of knowledge about a quantity, the Principle of Maximum information Entropy (PME) [99] is utilized. If, for example, one knows that the possible values of a quantity or parameter are contained in an interval, in accordance with the PME, this information is to be represented by a rectangular PDF. In uncertainty evaluation, this approach to representing information is termed "Type-B Method" [94]. Repeated observations are usually characterized by a Student t-distribution.

The ISO-Guide to the Expression of Uncertainty in Measurement [94] in particularly takes the expectation of a PDF expressing the information about a quantity Y as its best estimate:

$$y = E[Y] = \int_{-\infty}^{+\infty} \eta g_Y(\eta) d\eta \tag{4}$$

and the square root of the variance of the PDF is called the standard uncertainty associated with the above expectation:

$$u_y = \sqrt{\mathrm{Var}[Y]} = \left[\int_{-\infty}^{+\infty} g_y(\eta)(\eta - y)^2 d\eta \right]^{1/2} \tag{5}$$

For a given probability P a coverage interval (confidence interval) for the measurand is expressed in terms of an expanded measurement uncertainty $U = k_p u_y$, where k_p is a coverage factor that depends on P [94].

The interval:

$$[y - U, y + U], \tag{6}$$

then contains the true value of Y with probability P.

Both, in uncertainty evaluation and in measurement data fusion, the result is expressed by a so-called joint PDF for the measurand. In uncertainty evaluation, this joint PDF is obtained as Bayesian inference [99,175] from the existing knowledge by propagating the PDFs for the input variables $g_{Xi}(\xi_i)$ including the so-called model prior which is the Delta function of the (inverse) measurement model:

$$g_Y(\eta|q, I) = \int_{-\infty}^{+\infty} \cdots \int_{-\infty}^{+\infty} g_{X1}, \ldots, g_{XN}(\xi_1, \ldots, \xi_N), \; \delta[\eta - f_M(\xi_1, \ldots, \xi_N)] d\xi_1, \ldots, d\xi_N \tag{7}$$

where q is the measured values (observations), I existing information about the measuring process, f_M model of the measurement process [186,187].

Because expression (7) the Markov formula can be solved analytically for fairly simple cases only, in practice one uses Monte-Carlo techniques for propagating the PDFs [33,95].

Bayesian inference is based on the Bayes theorem [175]:

$$g_1(\xi|d_1) = K_1 l(\xi|d_1) \cdot g_{1*}(\xi), \tag{8}$$

where $g_{1*}(\xi)$ represents the state of knowledge about the possible values ξ of a measurand X_1 prior to the measurement; $l(\xi|d_1)$ is the likelihood describing the measuring process for this quantity X_1, and $g_1(\xi|d_1)$may be interpreted as the knowledge posterior to the measurement, i.e. after taking the observation(s) d_1 into account. Therefore, $g_1(\xi|d_1)$ might be interpreted as the degree-of-belief distribution for the measurand. K_1 is a normalization constant.

Bayesian fusion of various measurement results or of a measurement result $g_1(\xi|d_1)$ with any other measurement information d_2 represented by a PDF is simply carried out by applying Bayes theorem once again:

$$\begin{aligned} g_{12}(\xi|d_1,d_2) &= K_{12} l(d_1,d_2|\xi) \cdot g_*(\xi) \\ &= K_{12} l(d_1|d_2,\xi) l(d_2|\xi) \cdot g_*(\xi) \end{aligned} \tag{9}$$

Assuming that the two likelihoods or respective PDF are independent of each other, the joint PDF is obtained just by multiplying the likelihoods or PDFs:

$$g_{12}(\xi|d_1,d_2) = K_{12} l(d_1|\xi) l(d_2|\xi) \cdot g_*(\xi) \tag{10}$$

It should be emphasized that the above likelihoods characterize the state of knowledge of the measuring processes of a multisensor system.

In the case of the evaluation of repeated observations, the likelihood can be approximated by the frequency distribution of the observed data or, in case of only a few observations, by an appropriate data model distribution.

In case of non-statistical information, the likelihood might be described as state-of-knowledge PDF which can be obtained via the principle of maximum entropy (see Section 1.2). Necessarily, the linkage between the different sources of information to be combined has to be considered. This can be achieved by introducing a so-called model prior [115].

Therefore, information fusion by Bayesian inference is completely consistent with Bayesian measurement data and uncertainty evaluation; they use the same probabilistic approaches and the same mathematical tools.

3. Sensor technologies, their capabilities and influences on data fusion

Different sensor technologies are available for dimensional measurements. In addition to the tactile data acquisition, optical sensors and computed tomography are being used to an increasing extent. Fig. 4 gives an overview of established methods for dimensional measurements.

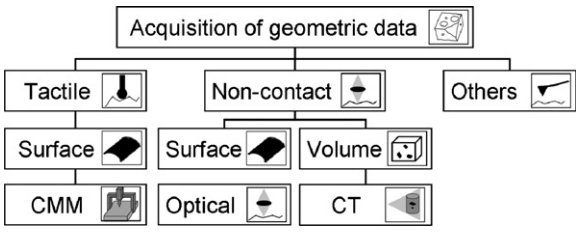

Fig. 4. Methods for data acquisition.

3.1. Optical sensors

Optical metrology can acquire a high density of point data from the surface with rapid speed. Its non-contact nature makes it suitable to capture the surface of flexible and soft materials [171]. However, optical methods also have their limits, such as lower accuracy compared to tactile sensors, occlusion and limited viewpoint, as well as sensitivity to optical surface conditions such as specular surfaces. The data acquired by optical sensors is often noisy and imperfect and can show redundancy in some areas and missing data in others [194].

To measure geometrical and dimensional quantities, usually optical distance sensors are used. They can be classified as point-sensors (1D-sensors), line-sensors (2D-sensors) and areal-sensors (3D-sensors) [106,140]. Areal-sensors, which only scan the surface vertically and do not measure for example undercuts, are classified as 2.5D-sensors. The achievable accuracy of a given optical sensor strongly depends on the interaction between the sensor principle and the surface material or the geometric structures which have to be measured. The sensors are characterized by naming the physical principle of the probing effect.

3.1.1. Triangulation sensors

Triangulation sensors are frequently employed for in-process metrology, reverse engineering and coordinate metrology, e.g. for the measurement of complex freeform surfaces such as car bodies in the automotive industry [162]. The measuring areas of common laser triangulation sensors (1D-sensor) range from mm to cm [171]. An extension of the triangulation principle is known as light sectioning (2D-sensor), where – instead of a single spot – a line is projected onto the specimen. If 1D- and 2D-sensors are not sufficient (e.g. for the sampling of complex surfaces with a high point density) fringe projection (3D-sensor) can be applied [200]. To clearly evaluate the height information a sequence of different fringes is projected onto the surface (e.g. "Graycode") which makes a reliable correspondence between the projected and detected fringes possible. Additionally, using the "Phaseshift" algorithm a higher resolution and measurement accuracy compared to the 1D- and 2D-triangulation sensors can be achieved. The measurement volume of common fringe projection systems ranges from 1 mm × 1 mm × 0.3 mm to 2 m × 2 m × 0.5 m with measurement uncertainties of 0.005–0.3 mm [174]. Uncertainty contributions depend on factors such as phase measuring errors, the optical aberration of the lenses and the used calibration method used, in terms of "black box" or "model based" approaches.

3.1.2. Deflectometry

Painted car body parts as well as optical devices have specular properties, which require special measurement approaches for inspection. In contrast to the inspection of matte surfaces, neither direct evaluation of grey scale pictures nor triangulation can be used. To allow a three-dimensional measurement of specular surfaces a measuring principle called deflectometry can be applied, where with the help of a data projector a series of stripe patterns is generated on a projection screen. The reflection of these patterns at the surface of the object is observed with a digital camera and is transferred to a computer for further processing [87].

3.1.3. Confocal microscopy

In confocal microscopy, only points on the workpiece surface produce high intensity peaks which lie exactly in the focal plane. Light emanating from regions above and below the focal plane is impeded by pinholes in the optical path. The topography is measured by vertical scanning and detecting the intensity peak for each camera pixel. This enables the confocal microscope to achieve high axial resolution and to increase the contrast and improve the signal-to-noise ratio of the final image. For sampling the workpiece surface, different techniques utilizing pinholes on a rotating disk, scanning mirrors, arrays of micro-lenses or digital-mirror devices have been developed. The measuring area and the lateral as well as

the vertical resolution depend on the numerical aperture of the objective.

3.1.4. White light interferometry

In white light interferometry, common microscopes with an integrated interferometer (i.e. Mirau or Michelson interferometer) are used. To decrease the interference range and to enable the measurement of rough technical surfaces, a broadband light source with a small coherence length is used. With a mechanical shift in the vertical direction the topography of the surfaces can be reconstructed by evaluating the recorded correlograms. Commercial white light interferometers achieve vertical resolutions down to 0.1 nm and vertical measurement ranges from 200 nm to a few mm, while the lateral measurement resolution depends on the numerical aperture of the objective. Uncertainty is influenced by "phase jumps" caused by inhomogeneous workpiece material, vibrations from the environment and "bat wings" if different correlograms interact.

3.1.5. Focus variation

In a distance sensor based on focus variation [39] the area of the workpiece to be measured is imaged onto a CCD-camera by a microscope objective. An image stack is recorded while a *z*-axis translation stage varies the distance between the objective and the workpiece. In the evaluation process, for every pixel the *z*-position with the highest local contrast is determined. This sensor determines in addition to other sensors the color distribution of the workpiece.

With the areal-sensors based on confocal microscopy, white light interferometry and focus variation it is possible to measure 2.5D topographies by uniaxial scanning.

3.1.6. Further types of widely used optical sensors

In addition to these 2.5D or 3D sensors there are other 1D sensors which are applied in dimensional metrology, including laser autofocus, video-autofocus, sensors based on chromatic aberration and conoscopic sensors. Also laser scanners are widely used. They have a very high data rate, and good resolution.

3.1.7. Image sensor

Image sensors are mainly used in machine vision for quality control and process monitoring. They are applied to solve problems of a visual nature where human vision could be somehow damaged or stressed, for example by repetitive/quick inspection tasks or when automatic inspection is required (presence/absence of features) [166]. Image sensors capture an object by optical projection of the reflected light with an acquisition system. They produce two-dimensional intensity data which always possesses the same dimension [11,71].

Image sensors have a geometrical resolution starting in the submicrometer range which can be increased by applying subpixel methods. Thousands of data points can be acquired simultaneously over a large spatial range, without moving the optical head. The problems associated with using intensity images can be divided into two classes: geometric constraint problems and radiometric constraint problems. Geometric constraints include visibility, field of view, depth of field, and pixel resolution. The radiometric constraints include illumination, specularity (glare), dynamic range of the sensor, and contrast.

3.2. Tactile sensors

Tactile probing systems are usually applied in cases where surface measurements allow or require lower point data density, such as prismatic workpieces, surfaces with a known CAD model or a shape without large variation. Their measuring ranges span from about a micrometer to several millimeters with an operation in one, two or three dimensions. In a special case 2.5 dimensional probing systems are planar sensitive and have only limited measuring range perpendicular to this plane. Tactile probing

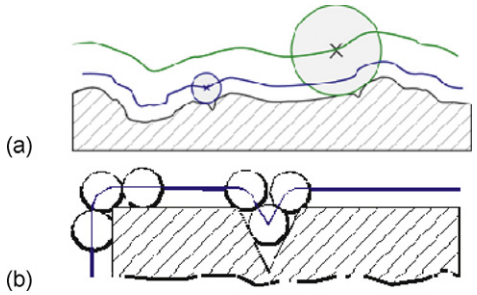

Fig. 5. Influence of tactile probing system [197].

systems are generally slow in acquiring points compared to optical systems, but show a higher accuracy. An overview of probing systems for coordinate measurements is given in the STC P Keynote paper 2004 [197].

The working principle of tactile probing systems is based on a mechanical interaction with the workpiece. There are two modes, discrete-point and scanning mode, which are differentiated. In discrete-point probing the measurement of surface points is done by lifting off the sensor between any two measurements and touching it again at the next point to be probed. A disadvantage of this method is that it may take a long time for each point as the process of approaching the surface and withdrawing has to be repeated for each point to be probed. In scanning mode the touching element is guided on a line along the surface while a set of coordinates are sampled in a time sequence, the tip ball is all the time in contact with the surface. In scanning mode more points per unit time can be measured, while their measurement uncertainty is higher than with discrete-point probing.

The interaction with the workpiece causes a mechanical filtering of the surface as shown in Fig. 5a. Surface zones might not be measured if the tip ball has more than one contact point and sharp edges or peaks might lead to smoothed approximation of the surface (Fig. 5b).

3.3. Computed tomography (CT)

In an industrial CT measurement system the workpiece is positioned between the X-ray tube and the flat panel area detector. A stack of X-ray projections of the workpiece is recorded in different rotational orientations using a rotary table. In a reconstruction process, 3D volume data is calculated. This data consists of a regular 3D grid of the quantized local material density which is discretized in small volume elements (voxels). The workpiece surface is finally calculated from the local material density distribution by threshold operations. Alternative CT configurations (2D CT systems) use a fan beam and an X-ray line detector. With these configurations a time-consuming synchronous vertical movement of the X-ray tube and detector is necessary to measure enough slices of the workpiece. On the other hand, these systems deliver, in most cases, measurements with smaller measurement deviations, especially when larger parts are measured.

The attractiveness of CT lies in the fact that it gives, in its common performance and within a short period of time, precise quantitative information on the whole structure of a body without destroying it. This factor has made CT very interesting and appealing for testing and inspecting manufactured workpieces like engine blocks, gear boxes or even injection nozzles [171]. Important quantities which influence the performance of CT are the relative distances between the source, the object to be measured and the detector, as well as geometrical errors of the mechanical axes. In addition, the size and the shape of the X-ray focus, the X-ray spectrum and the energy-dependent absorption of the object have an influence. The dimension, the geometry and the material composition of the object comprising surface or interface properties such as roughness are influences specific to the object under study. Further influencing quantities are the lateral resolution of the detector, the detector properties (energy-

dependent sensitivity, signal-to-noise ratio and dynamics) and the pre-processing of the detector signal. Last but not least there is the influence of the tomographic data reconstruction and the post-processing of the voxel data (e.g. threshold process for surface extraction) [8,165].

3.4. Scanning probe microscopy

Compared to optical sensors scanning probe microscopy can achieve atomic resolution. It relies on a mechanical probe for the generation of magnified features in three dimensions. A very small zone of interaction implemented by a small probe tip (ideally one atom) is scanned across the measuring range. Various kinds of interactions are possible, e.g. mechanical (atomic force microscopy), optical (near-field scanning optical microscopy), magnetic (magnetic force microscope), quantum-electric (scanning tunneling microscope) and thermal (scanning thermal microscopy). They are applied for measurement of surface roughness, topography and material properties with the advantage of very low forces acting on the workpiece, resolution in the sub-nanometer scale and simultaneous measurement of topography and material properties. Restrictions are caused by the accessibility of the scanning tip to the surface and the conventionally very small measuring ranges (typically 10 μm in vertical and 50 μm × 50 μm in lateral direction) and working distances [198,199].

Data fusion methods in the field of dimensional metrology have been applied for atomic force microscopes (AFM). An AFM has three modes of operation, contact, intermittent and non-contact. The intermittent mode is generally used for looking at soft specimens since it is less likely to cause specimen damage than the contact mode. Contact and intermittent contact mode achieve higher resolution than that of the non-contact mode.

Scanning probe microscopies are very sensitive to vibration, electrostatically forces and capillary forces caused by a thin water film. Such measurements should be carried out under a protective cover in a climate-controlled room.

3.5. Sensor capabilities and influences

Even though tactile and optical sensing technologies are widely used in data acquisition in dimensional metrology, it has been shown that each technique has its own characteristics and applications.

While fusing data sets characteristics such as resolution and measuring ranges (Fig. 6) have to be considered. On the other hand due to the different measuring techniques and their physical working principles different interactions between the workpiece and sensor occur and different surfaces are captured. Factors which influence this can be shape and roughness of probing systems, the direction of probing or the optical and mechanical characteristics of the workpiece.

While fusing two data sets the question arises how they are to be combined.

4. Examples of data fusion in metrology

The theoretical origins of data fusion date back to the late sixties, although a broad application of these techniques did not take place until the early eighties. In the mean time, the bibliography on data fusion has become very extensive, and applications to several fields have been reported, such as robotics, pattern recognition, medicine, non-destructive testing [17,36,42,45,55,56,72,100,118,119,127,179] geo-sciences, reconnaissance and finances [70]. In the following, areas of application of multisensor data fusion in dimensional metrology are presented.

4.1. Image fusion

Image fusion is the process of overlaying and fusion of images (two or more) of the same scene taken at different times, from

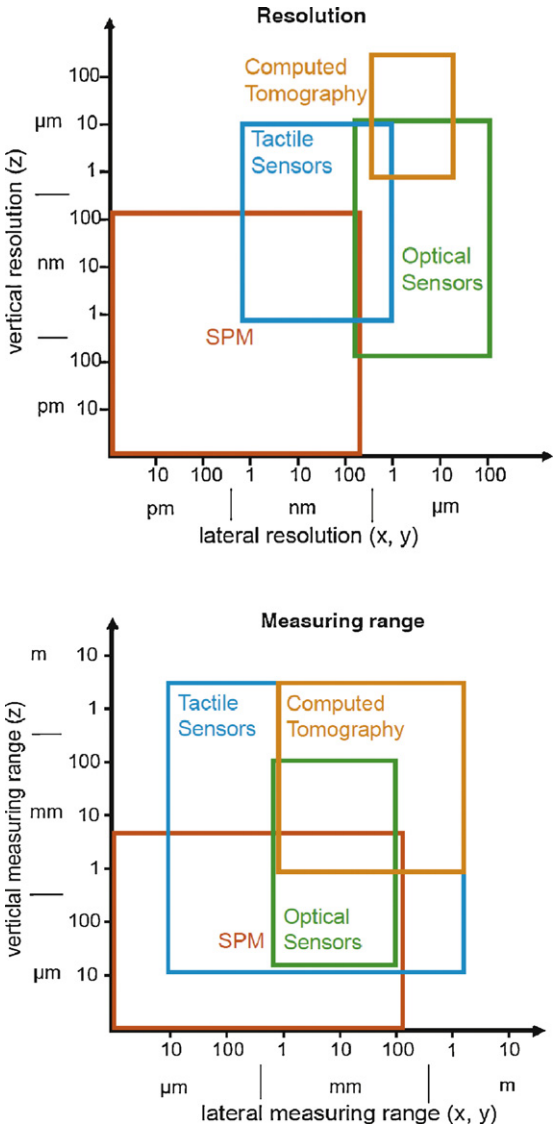

Fig. 6. Typical resolution and measuring range plots for optical sensors, tactile probing systems in coordinate measuring systems, computed tomography and scanning probe microscopes.

different viewpoints and/or by different sensors. If camera position, camera orientation or reproduction scale are not equal for the images which have to be fused, above mentioned image registration methods have to be applied. In Section 2.2 an overview of registration methods for dimensional metrology was introduced.

4.1.1. Visual inspection

Measuring tasks in the field of visual inspection require high quality image data. The necessary quality is often achieved by applying image fusion methods across sensors, also called multimodal analysis. With one camera only it is often impossible to achieve a representation of sufficient visual quality. The reason for this is the manifold interaction between the illumination, the object and the observation optics on one hand, and the limited sensing capabilities of common 2D intensity sensors to measure the information-bearing light field on the other hand. Image optimization can be achieved by a multimodal analysis, i.e. fusing images of the same scene acquired by different sensors or taken with different illumination and/or observation parameters (e.g. illumination direction, structured illumination, camera position and orientation, spectral response, focus, etc.) (see Fig. 7). If the image acquisition is done with the same sensor, but with at least one varied acquisition parameter the sensors are also called "virtual" sensors [83].

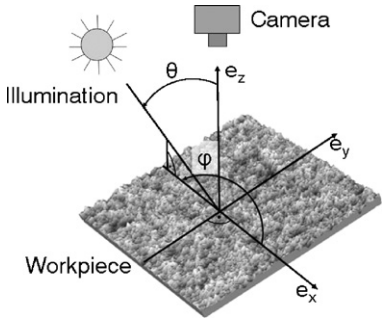

Fig. 7. Variation of illumination and/or observation parameters in image series as data foundation in image fusion. Based on [84].

To enhance the image quality, fusion on the pixel level is applied. By varying the illumination direction a series of images is captured using homogeneous and "virtual" sensors [79,206]. The useful information is concentrated in one or a few images of the series. Complementary fusion approaches select the useful information in each image. The data are transformed by coding the images in the series with the highest local contrast and finally fusing by globally maximizing the local contrast as quality degree [83,85]. Compared to the single images of the series more details of the surface can be detected on the final image. Another universal approach for complementary image sensor data is to formulate the fusion problem with an energy function [150]. The desirable characteristics, postulates, prior knowledge and further assumptions regarding the image series are described by the summands of this function. Some advantages of this approach (compared to the fusion processes introduced in Section 2.3) are its generality as well as the possibility to incorporate additional information and constraints by simply adding further energy terms. The optimal fusion result with respect to the assumptions met is obtained by minimizing the energy function (see Fig. 8).

To generate images of superior quality, a series of exposures, in which the shutter time is varied, can be recorded. In [11] this is applied to improve the signal to noise ratio (SNR) of images of technical workpieces. As such workpieces may show a significantly higher dynamic range than image sensors, typically 8–12 bits, dark areas typically are imaged with a low SNR or even disappear in the background noise, whereas bright areas of a scene will suffer from an undesired saturation degree. By varying the shutter time, every point will have a satisfactory SNR in at least one exposure of the series. In the following fusion stage, those regions showing the best SNR are combined to result a high SNR overall.

To improve the extraction of image features or enable access to features that are distributed over an image series fusion is applied on feature level. It requires the preceding extraction of relevant features by means of local operators such as structural tensors. Fig. 9 shows images of sealing surfaces which were acquired by varying the illumination azimuth. Whereas points in the intact groove texture show two intensity maxima during one rotation of the light source around the sensor due to the reflection on the groove flanks, intensity curves in the defect regions show no distinctive intensity maximum. The features can be distinguished

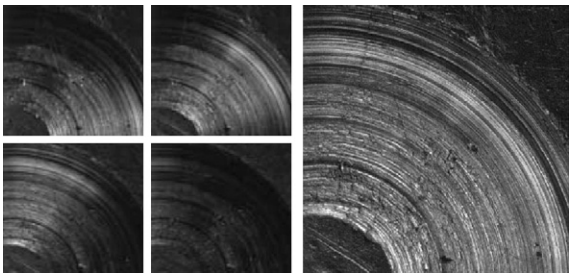

Fig. 8. Image fusion on pixel level. (left) Image series, (right) combined areas with highest contrast to enhance the visibility of grooves on a metallic surface [150].

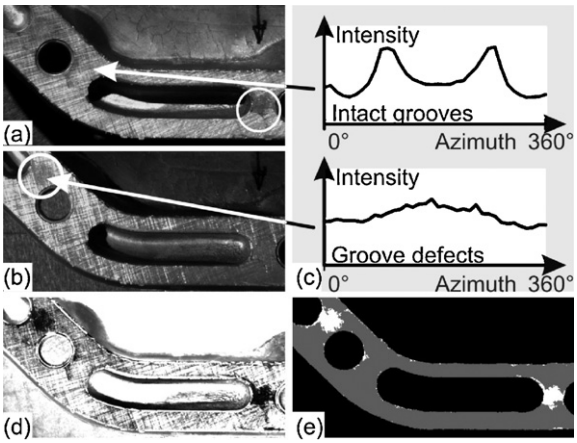

Fig. 9. Image fusion on feature level for the inspection of defects on ground surfaces. (a) and (b) Image series with varying illumination azimuth, (c) typical intensity curves for the intact groove texture and defect regions, (d) variance analysis, defects are presented dark, (e) fusion result [85].

by techniques such as variance analysis (Fig. 9d), harmonic analysis or analysis of the periodicity of measured intensity. A classification of intact groove texture and groove defects is undertaken according to a set threshold. The result of the classification is also the fusion result (Fig. 9e) in which the intact groove texture is shown as grey while the groove defects are shown as white [206].

To detect defects on machined surfaces, e.g. painted car doors or on membranes of pressure sensors the inspection can be performed in a similar way, by recording an image series of the surface by using binary patterns. The grooves reflect the pattern intensities which are bi-directional, perpendicular to their own local direction. If the patterns perpendicular to the course are dark, dark areas should be expected for an intact texture. On the other hand bright regions emerging from a dark groove texture indicate local defects. Harmonic analysis of the signals enables extraction of a feature image that robustly defines local surface defects. An analysis of the image intensities at each location of the image is carried out, which allows the determination of a feature image as result of the image fusion. Similar to the examination of the membranes of pressure sensors, defects on painted car doors can be detected [151].

4.2. Fusion of image data to achieve dimensional information

4.2.1. Depth from focus

The 3D-distance sensor based on focus variation presented in Section 3.1 is one example of image fusion on pixel level, where dimensional information is gained due to the fusion process. Useful information is distributed over the whole recorded image series while the distance between the objective and the workpiece is varied (see Fig. 10). Only the evaluation of all images allows for statements on the desired properties to be made. In a comple-

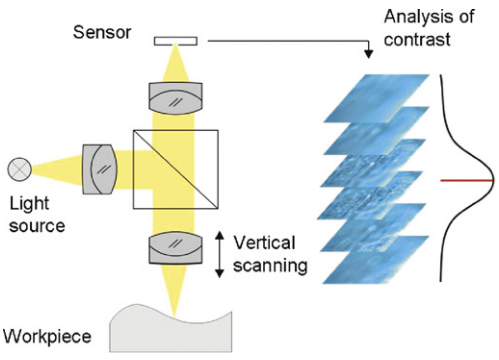

Fig. 10. Depth map based on focus series (depth from focus) [174].

mentary fusion approach the "number" of the image, which presents the vertical position of the focus, with maximum contrast is transferred into the result, to gain a depth map of the workpiece. The additionally gained color information facilitates the fusion process when overlapping measurement fields are stitched.

Similar fusion approaches are applied in white light interferometry (height information is achieved by evaluating the intensity curve or the phase information of the white interference signal) and confocal microscopy (vertical position of the image with maximum intensity is transferred to the resulting depth map) [174].

4.2.2. Shape from shading

Reconstruction of the topographies is also possible by applying techniques such as 'Shape from Shading' [30]. An image series is captured with virtual and homogeneous sensors in a setup consisting of different illumination sources and a fixed camera as presented in Fig. 11a. The procedure of reconstructing the topography works in two steps. In the first step the gradients in the *x*- and *y*-direction have to be calculated from captured greyscale images. In the second step, a height map is derived by integration of the gradients. At least three images for different light directions are required to calculate the gradients [88]. Improved results and an estimation of measuring errors are achieved if more than three pictures are captured. The topographical map is calculated by integration over the gradients as described in literature [1,88]. Different algorithms in 'Shape from Shading' following algebraic approaches as well as methods involving an energy function of Bayesian approach are presented in [30]. One example of the application of 'Shape from Shading' is the analysis of positions and heights of braille points on medicament boxes (see Fig. 11b) [184]. It is also used for the automated treatment of human skin diseases curable by UV radiation [109]. Based on this three-dimensional information created by the 'Shape from Shading' sensor and a color image of the same area, the diseased areas are automatically detected. Using this healthy/diseased data an irradiation plan and NC program for a scanner guided excimer laser is generated. Then, the generated NC program is executed by a laser scanner and a laser beam is guided across the surface to solely irradiate the diseased skin [73].

4.2.3. Photogrammetry

Photogrammetry is a metrology technique in which the shape, size and position of objects are determined from cross-domain fusion of measurements made on two-dimensional images. It can also be classified as a passive triangulation principle, where three-dimensional coordinates of points of interest are calculated via optical triangulation from two or more images taken from different locations. Close-range photogrammetry, commonly called vision metrology, is in the main method for using this to generate the three-dimensional coordinates of a point in object space. In a typical multi-station photogrammetry network, as presented in Fig. 12, there may be several images and many redundant observations. This leads to an overdetermined system of equations that is most often solved by least squares estimation. The camera interior geometrical parameters such as principal focal length, centre of image plane, lens distortion and the position and

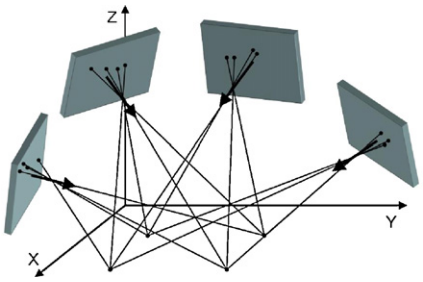

Fig. 12. Multi-station photogrammetry setup [177].

orientation parameters for each image needs to be known a priori. The image position and orientation parameters are together known as the exterior orientation and consist of the XYZ coordinates of the perspective centre and the three rotation angles between the image- and object-space coordinate axes. In the mid 1950s, a solution was developed in which the point coordinates and exterior orientation parameters were determined simultaneously. This solution is known as bundle adjustment [49,171]. After calibration of a system with the bundle adjustment technique three-dimensional local images are processed, which must be registered to obtain a final global point cloud of the object. Surface and feature based algorithms, as introduced in Section 2.2 are then applied. The area based matching takes advantage of correlation coefficient maximization and least squares minimization, while feature based matching exploits all algorithms extracting features as points, lines and areas [21].

Photogrammetric systems that capture the geometry of free-form surfaces from 3D objects of design models and for quality inspection in prototype or series production have proven to be very important in industrial applications [49,171,188]. Measurement of a double-decker train by means of photogrammetry is presented in [37]. Encoded markers are placed on the train and photographed from different directions and heights. A software algorithm is then applied which recognizes the encoded marker (features) automatically. To calculate its position, a marker has to be visible in multiple images.

Further examples are the measurement of freeform surfaces of railway concrete sleepers and the calculation of track and rail seat dimensional tolerances applying a stereometric system, based on two cameras with calibrated positions towards each other [2]. The combination of depth from stereo and depth from focus also can lead to robust 3D information [64].

There are several vision coordinate measuring setups. One example is a system which consists of a specially designed light pen with point shaped LED light sources which are aligned in one line with the probe stylus and a high-resolution CCD (see Fig. 13a). On the basis of knowing the positions of the light sources and the probe stylus the 3D coordinates for the centre of the probe stylus can be calculated. The disadvantage of such systems is the uncertainty in direction of the optical axis of the camera lens. It can be shown, that the CMM measuring precision is improved when such a dual CCD-camera vision system is applied and additionally the system's measurement range is enlarged.

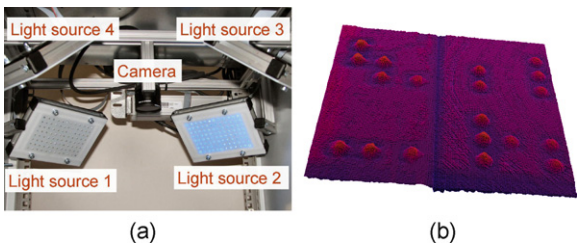

Fig. 11. Automatic inspection system based on 'Shape by Shading': (a) setup of illumination and camera (b) analysis of braille points on medicament boxes [58].

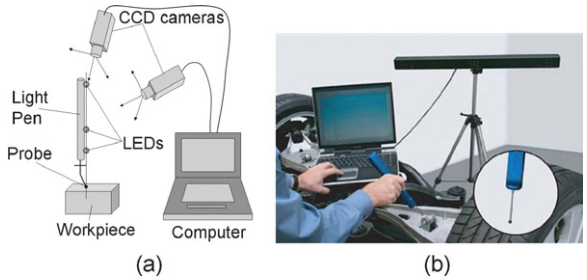

Fig. 13. (a) Setup for a dual camera 3D coordinate vision measurement on base of [116] and (b) similar setup applied in the industry [157].

During measurement the touch trigger probe contacts the object measurement surface and the image of the light sources is captured by dual CCD cameras, whose optical axes are perpendicular. The coordinate rotation and translation between the two camera coordinate systems is calibrated (prior knowledge). The two cameras' measuring results are processed with corresponding weighted values. Experimental results of such a setup showed the axis orientation errors were eliminated and a better stability and precision with an uncertainty of ±0.1 mm in the distance of 2 m [116]. Similar setups apply infrared technology to detect the position of the light pen and the probe stylus (see Fig. 13b). To enlarge the measuring range further, two dual sensor setups can be combined [157]. A further method presented in [91] is to focus an infrared beam onto the surface and scan the small light spot.

4.2.4. Fringe projection systems

For the three-dimensional shape measurement of complex structures fringe projection systems are applied [71,112,117]. The data sets are used to evaluate form characteristics or to compare the data set with a CAD model. Fringe projection can be applied in mobile systems for example to digitize freeform surfaces or in coordinate measuring machines. Often, the measurement objects are bigger than the measurement area of the sensor or too complex to be captured in one single measurement. In a complementary integration partial views are taken from different sensor positions and registered and fused across the domains [148]. Problems such as shading can be solved with such a setup and the accuracy of the measurement can be improved (see Fig. 14).

All the local 3D coordinates are transformed into the global coordinate system and patched together using, for example, a least squares fit method. There are several approaches to determine the relationship between the global and local coordinate system: (1) accurate mechanical location and orientation of the sensor (local coordinate system), (2) optical tracking of the location and orientation of the sensor using active or passive targets attached to the sensor, and (3) photogrammetry of markers accurately fixed in the object field and hybrid methods [21].

A solution for approach (3) determines the shape of a partial view by a combination of the phase-shift method for fringe evaluation and a photogrammetric triangulation to calculate the 3D coordinates related to the sensor coordinate system [155]. The problem of matching the partial views to each other is solved by transforming each sensor position and the relating point cloud of the shape in a global coordinate system by photogrammetric matching of the reference targets. According to this strategy, point clouds taken from different sensor positions can be transformed into the global coordinate system with very high precision.

4.2.5. Deflectometry

From the directly measured deflectometric data no unambiguous reconstruction of three-dimensional shape is possible. Different approaches allow for reconstruction with the aid of additional knowledge or the fusion of several measurements [87,102]. For the reconstruction of 3D specular surfaces from noisy sensor data the Bayesian technique, applying *a priori* knowledge, is used [43]. The fusion of *a priori* information allows smoothing noisy regions while simultaneously maintaining geometrical features, as the estimated surface form can be represented by a CAD Model. Fig. 15 shows a simulated deflectometer measurement result which shows a spherical elevation. The simulated height data were overlaid with equally distributed random noise. If the form of the surface cannot be described with one single CAD Model (e.g. parts of a car body) *a priori* knowledge about the position of the parts relative to each other can be used to identify certain components, before their geometrical data is included in the overall measuring process.

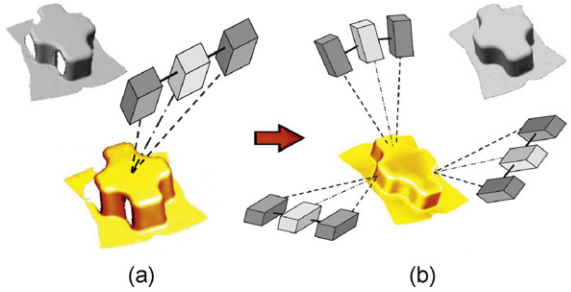

Fig. 14. (a) Inspection using one measurement: parts of the object are not detected or only with bad quality (red areas) captured. (b) Gain in information and improved accuracy with three measurements [201].

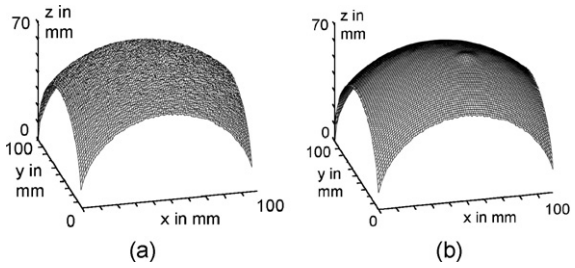

Fig. 15. (a) Simulated sphere with spherical elevation and equally distributed random noise; (b) smoothed data [87].

4.3. Tactile and optical multisensor coordinate metrology

4.3.1. Integration in coordinate measuring machines

The reduction of the lead time in reverse engineering, and the increased requirements in terms of flexibility and level of automation of the whole digitization process have resulted in a great deal of research effort aimed at developing and implementing combined systems for the reverse engineering based on cooperative integration of inhomogeneous sensors such as mechanical probes and optical systems [4].

The optical system can be a simple video-camera, which acquires the global shape information and provides the CMM with the exploration paths of the tactile probe or other sensors [20–25,65,177,178]. Such systems, of which two are to be described in more detail, combine the strength of a vision system, the ability to quickly generate global information, with the strength of a touch probe, the ability to obtain highly accurate measurement information (see Fig. 16a). The part to be measured can be placed anywhere in the camera's field of view. Visual tracking is used to provide an estimate of positions of features of interest on the part. Fig. 16b shows the detected features on a piston ring. The information generated by using the vision system is fused with data generated by the machine scales and the probe. The fused information is used to guide the movement of the touch probe as it performs an inspection scan across the surface of a part. This allows parts to be measured even if an accurate *a priori* model is not available. All the vision data are represented in 2D image coordinates. Probe data are expressed in a 3D coordinate system relative to a pre-defined origin relative to the CMM table. Visual feedback to the system consists of updates of the 2D distance between the probe and the nearest edge. Both the current position and the intersection point on the edge are updated during each processing cycle. The world model fuses the visual information with the 3D position and velocity information supplied by the CMM in order to predict the 3D distance remaining between the probe and the part's edge. Using this real-time vision, the probe can be guided to features of interest, and probe measurements can then provide the inspection data [137].

An intelligent integration of the information from the optical and the contact sensors on the signal level allows the rapid reconstruction of objects of complex geometry [19,162]. Additionally a competitive fusion approach results in a higher accuracy for the digitization of the object. The starting point is the acquisition of a number of clouds of points using the 3D vision system. Each one provides initial dimensional information about

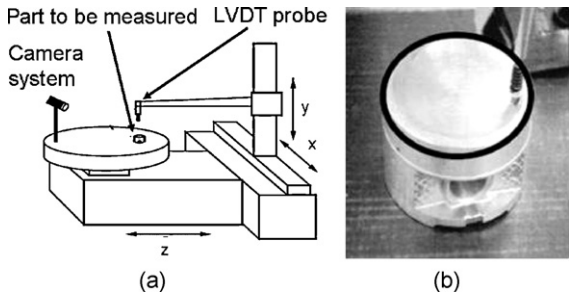

Fig. 16. (a) CMM probe and camera, (b) piston [137].

the object. The initial CAD model of the surface is then determined to be used as first approximation for CMM programming. The *a priori* knowledge of a "rough" surface model allows efficient programming of the scanning and digitizing path of the CMM mechanical probe, with a reduction of the number of touch points. The measured data are then imported back to the CAD environment and used to produce the final, accurate CAD model (see Fig. 17).

One- and two-camera based vision systems or even stereo camera setups are, as monitoring elements, also integrated into production systems. They control the position of the workpieces as well as they provide information for the mechanical probing [44].

Instead of a vision system laser scanner data can also be applied [47,97,98]. A sensor approach to reverse engineering based on the application of a laser line sensor is presented in [16]. With its high data sampling rate the sensor is suitable to detect the large point cloud data files required to define freeform surfaces, whereas a CMM touch probe's accuracy is used to precisely define the boundary of bounding contours. Both sensors are mounted on the *z*-axis arm of a computer controlled CMM. The data produced by each sensor is referenced to an identical origin and axes in the work volume of the CMM. Therefore the laser sensor and touch probe data are subsequently referenced to the same coordinate system. Typically, a cloud data set is obtained, by the laser sensor head, from the entire object surface and then transferred to the workstation where the overall cloud data file is constructed. The viewing position and orientation of the range sensor head can be adjusted to gather data from as many views as necessary to completely define the object. Each view is treated as a separate record, from which the overall cloud data file is composed. The touch probe data from each surface patch boundary is acquired and accumulated in the CMM personal computer before being transferred to the workstation. The patch boundary data is integrated with the correspnding cloud data file. The fitting process uses the boundary data, collected by the CMM, to define the four bounding B-spline curves for each patch. These curves remain spatially fixed, during the subsequent patch fitting, thereby ensuring the physical edges do not move [16]. Such a multiple sensor integration can capture metrologies with 2D and 3D data acquisition by tactile and optical sensor techniques. Further setups have been introduced which even integrate 1D acquisition possibilities, such as a chromatic confocal sensor and therefore cover the macro as well as micro level [209].

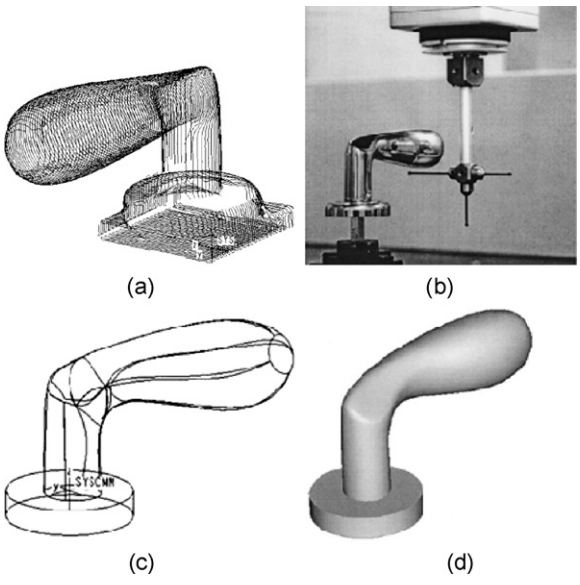

Fig. 17. Reconstruction of door handle (a) Fused scan curves of point clouds acquired with an optical sensor, (b) tactile measurements on the CMM, (c) partial reconstruction after tactile measurement of the functional surfaces, (d) final shading of the handle CAD model [19].

4.3.2. Integration in machine vision systems

The inspection process of machine vision systems can be optimized in terms of time and accuracy by integrating cooperative sensors. One such example is given in [168]. The presented system for inline inspection of textile structures positions and aligns fibre-reinforced plastic structures automatically. The developed method combines an image processing sensor for the robust detection of the local fibre orientation and a light section sensor for the determination of the contour position of textile preforms. The method used to detect the local fibre orientation does not only allow a measurement of the alignment of the textile layer, it can segment each layer and thus calculate roughly its contour's location. This is used as the scanning path for the light section sensor, which is applied in the subsequent step to measure the contour more accurately. After fusion of all this information, the system defines position and alignment of each textile layer as well as measuring geometrical parameters. Additionally it controls the 3D deformations of each textile layer during the drapery process (see Fig. 18).

4.3.3. Stitching

High precision measurement of large and complex technical surfaces, which have a large measurement area requirement from a homogeneous sensor, can be captured by registering (stitching) single measurements together. The registration of the measurements is based on the positioning of the sensors towards the measurement object. The knowledge about the sensor positions is gained in the calibration process. During coarse registration this knowledge is used to transfer the single measurments into one data set representing the digitized workpiece. To minimize the remaining deviations the iterative clostest point (ICP) algorithm is applied [207]. The automotive industry uses such systems for reverse engineering of components such as steel sheet pieces. The components are captured according to the measurement area of the CMM and then fused across domains. Every steel sheet piece needs more than 20 single views which are transformed into the coordinate system of the CMM and are finally fine registered (Fig. 19).

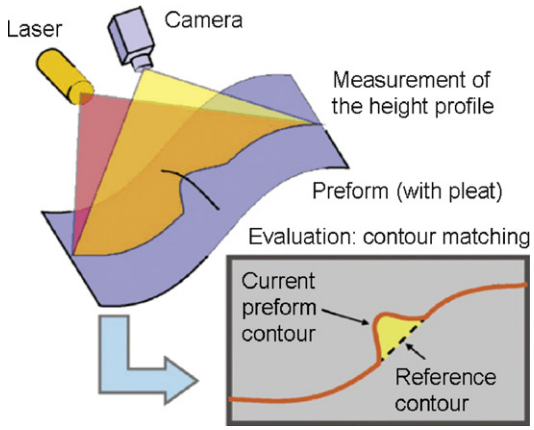

Fig. 18. Sensor integration in machine vision system for the detection of 3D deformation errors [168].

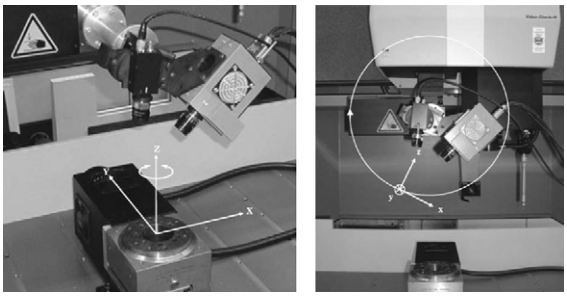

Fig. 19. Fringe projection system using the accurate mechanical location and orientation of the sensor to determine the relationship between the global and local coordinate system [207].

Similar systems, integrating an atomic force microscope with a coordinate measuring machine, are designed for topographic characterization of fine surfaces on large workpieces [77,78,125,191].

Multisensor data registration and fusion by using the capabilities of exact positioning enables the stitching of adjacent measurement areas without complex registration algorithms and independent of the sample topography [105].

Such exact positioning can be achieved with the nanopositioning and nanomeasuring machine (NPM) in which in contrast to conventional coordinate measuring machines the sample is moved instead of the sensor [96]. Sensors are fixed in a way that their working point is located in the Abbe-point. The integration of white light interferometry into the NPM machine enables it capturing samples whose lateral extensions exceed the field of view by stitching height maps from several single measurements at adjacent positions. Because of the capabilities of precision positioning the field of view can be exactly aligned for each measurement without complex registration methods. This method also works if the topography of the sample is homogeneous. The matching of the height maps requires the calibration of the sensor. The lateral relative transformation parameters from the sensor to the machine coordinates can be determined by registering a list of pass points between two images of the same grid structure which has been captured at different lateral positions. The assignment of the pass points between the two images is done using the nearest neighbor principle, which assumes that the transformation parameters are roughly known beforehand. Fig. 20 shows the measurement of the PTB layer thickness standard SH70 which was captured by stitching height data maps from 64 single measurements [105].

4.3.4. Multiscale measuring

The advantages of different sensor concepts (measuring principles) can be well combined by cooperative integration of inhomogeneous sensors with different resolution and applying multiscale measuring and verification strategies. Of importance is the overlapping of the scales of the applied sensor types. Examples of such setups consist of, e.g. a confocal microscope, a confocal point sensor and a conventional camera for 2D vision data [210] or a high-resolution image processing sensor with an AFM [153].

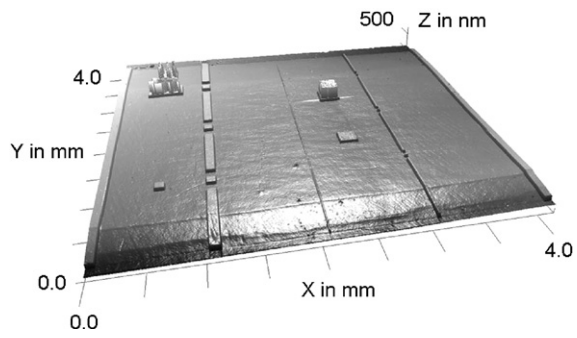

Fig. 20. 3D visualization of a measured PTB layer thickness standard SH70 (stitching of 64 fields of view, more than 21 million data points) [105].

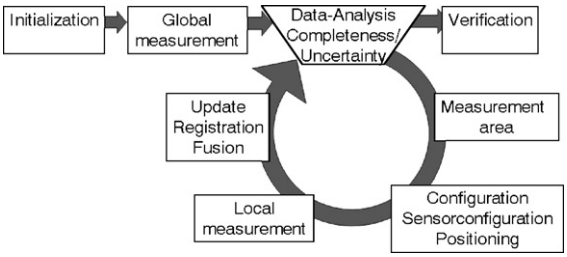

Fig. 21. Course of action for a multiscale measuring process on base of [205].

A proposed course of action for multiscale measurements is presented in Fig. 21. After the initialization of the system, the measurement object is captured globally to achieve a complete characterization of the object, but with restricted resolution. The measurement data is then analyzed and the information content is evaluated. However, further local measurements are required if there is not enough information for verification. The local capture of the surface includes the selection of the measurement area, the configuration of the sensor and the update of the measurement data set. After each addition of data, the interim object reconstruction is compared to the requirements of the measurement task. The objective is to apply time-consuming, high-resolution methods of measurement only to a limited set of critical positions, thus reducing the total measurement time. Goal of the update is to combine all available data about the measurement object in one data set. Feature and surface based methods are applied for the registration process. The two-stage process of the affine transformation (features on the surface are evaluated and then correlated) is used for the registration of surfaces showing significant features. Surface based methods such as the ICP algorithm are implemented for measurement data without deterministic features [205]. An estimation of the corresponding uncertainty is stored with each measurement point. The result is a point cloud that implicitly defines the object as a parametric surface.

There are developments, which integrate sensors with different measuring ranges and resolutions to visualize a large area of a workpiece in order to rapidly select a region of interest for a local SFM measurement. An optical system is used to obtain quantitative dimensional or even analytical information from the object. Measurement time can be reduced dramatically and the combined instrument bridges millimeter, micrometer and nanometer scales. The feasibility of combining an SFM with an optical interference microscope in single measurement is demonstrated in [192]. In another solution a compact SPM sensor head was directly included in an optical profilometer setup [180].

A setup to characterize micro-parts with low operator influence consists of a fringe projection system for global shape measurement and a white light interferometer for the characterization of the surface structure and wear, enabling a functionally oriented 3D-data evaluation. To execute the measurement of components such as cutting tool inserts, measurements in different positions are carried out by applying a positioning system. To determine the entire shape of the measurement object, it is kept on the positioning system and moved and rotated within the measuring fields of both sensors. The individual sets of measurement values are then transformed into one coordinate system in order to evaluate the dimensions of geometry. The coarse registration uses the knowledge of the coordinates due to the positioning system. For fine registration the ICP algorithm is applied. In addition the model can be used as basis for determining wear of a cutting tool insert in the machining process. For this purpose, measured 3D points of the cutting zone of a worn cutting tool insert, obtained by a white light interferometer, are registered with the data of a fringe projection system. The measurement data is combined in a 3D measurement cloud [196,202].

4.3.5. Self-optimized assembly based on multisensor systems

Developments in inspection systems have started to solve measuring tasks encountered commonly among small series production facilities. One application of such a multisensor system is in the self-optimized assembly of a micro-laser. The automation approach is based on a flexible assembly module, which makes use of robots for the positioning and assembly of laser components. The whole system is continuously updated with information from multiple sensors, namely a CCD-camera-based laser beam inspection system for monitoring the laser quality, a machine vision system for monitoring the fine positioning of the optical components, thermography and computed tomography for additional information (Fig. 22).

First the laser beam inspection system and position monitoring system for the optical components, which is assisting the robots in the components manipulation process, are integrated into a cooperative sensor fusion network. The laser beam optimization is firstly performed through its optical analysis during the fine positioning of the lenses through a robot. Next, the machine vision system monitors and determines, through image processing techniques, the accurate final lens position. The data fusion between the laser beam analysis and the machine vision system occurs in features and symbol abstraction levels, as the raw data provided by the sensors are not compatible, neither can be synchronized. Together the combined sensor data enable the system to learn the fastest way to find the ideal laser beam and to optimize itself.

When the fine positioning of the lenses has achieved its optimum, they must be definitely joined to the laser board by heating of glue elements under the optical components. Further integration of a thermographic camera, to monitor the component joining process and of computed tomography for generating a complete 3D model of the assembled micro-laser is planned.

4.4. Coherent and incoherent measuring techniques

4.4.1. Laser tracker

For systems subject to unknown or unpredictable variations, estimation methods that can adapt to these variations are required. An example [15,54] is the laser tracker, which determines the location of a target in three dimensions from measurements of azimuth and elevation angles and radial distance. The laser tracker is thus a portable coordinate measuring machine (CMM) that reports measured locations in spherical coordinates (r, φ, θ). To measure the radial distance a laser-interferometric transducer records changes in optical displacement. Both angle and interferometric displacement measurements are subject to random effects due to changes in the refractive index of air along the light path. The optical distance is increased by an increase in the refractive index while a uniform gradient in the refractive index orthogonal to the light path causes the light path to bend affecting the angle measurements significantly. To estimate the reflective index along the light path, in order to determine the appropriate correction factor for the interferometric measurements, pressure and temperature measurements are made at a number of locations. Even so, the lack of knowledge about the refractive index is a major source of uncertainty. It is difficult to assign *a priori* estimates of the relative uncertainties as the environmental conditions affect the angle and displacement measurements differently.

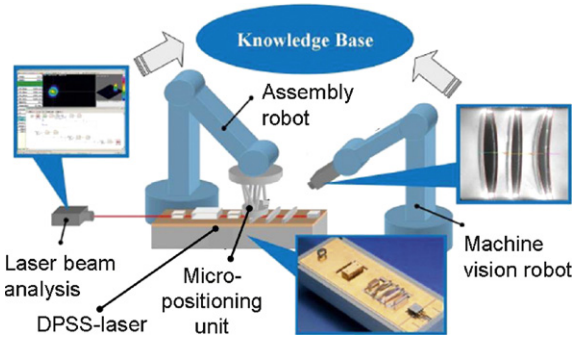

Fig. 22. Multisensor data fusion for self-optimized assembly of a micro-laser [167].

In order to improve the accuracy of such measurements multi-station systems, combining measurements from a series of fixed measuring stations, are assembled. The key elements of such a high-accuracy multilateration system are a number of laser-interferometer-based tracking stations, a wide-angle retro-reflecting target and a robust mathematical model to enable the spatial coordinates of point of interest to be determined from multiple displacement measurements. It is not necessary to know accurately in advance where the measurement stations are, relative to each other or relative to the target. The technique relies on data redundancy to deduce the unknown positions from the lengths measured [146]. For measuring the location of a point in space, ideally four measuring stations should be used simultaneously. It is also possible to use a pseudo-multilateration technique using only one single tracker [49,172]. Mathematical treatments similar to data derived from multiple sensors are introduced in [31,32,34,147]. Multilateration has been used successfully for dimensional metrology [68,89,146]. It is applied to measure parts too large for conventional CMMs:

Setup in a chain configuration [134] each laser tracker has its own coordinate system that is linked to the others through the measurement of common points. A point-set registration is used for finding the absolute orientation. After registration, any part feature viewable from more than one laser tracker, benefits from the fusion process. The redundant information of a particular feature gathered from multiple sensors is used to calculate a more accurate location for that feature. The error of each point is described by an uncertainty ellipsoid. The fusion algorithms presented combine multiple measurements by using a weighted average to give points with a better accuracy a higher weight.

Alternative schemes exist for laser tracking that do not rely on a combination of angle and length measurement. Mayer et al. [128] presented a multilateration system that relied solely on angular information. The LaserTracer, recently presented [172], uses multilateration or pseudo-multilateration to derive three-dimensional position from a tracking laser device that provides only displacement information from its interferometer. The advantage of this system is that it does not rely on the relatively coarse angular measurement of other tracking lasers.

Another example for merging measurement data captured from different views is a laser comparator for dimensional inspection presented in [90]. The merging process of the data captured from industry parts positioned on a turntable to assess the round view is based on the calibration of the rotation centre of the table.

4.5. Computed tomography

Due to the large number of influencing quantities (described in Section 3.3), CT systems often show significant errors which need to be corrected [28]. The improvement in accuracy is achieved by correcting systematic deviations of the CT data caused by different physical effects such as beam hardening, scattering and Feldkamp-effects. One improvement strategy to enhance the dimensional accuracy of industrial CT and to reduce the systematic measurement errors requires the use of calibrated reference standards [8]. Up to now, techniques have been applied for the correction of scale errors and the assessment of threshold values. A reference standard such as a ball bar, a ball plate featuring spherical calottes or a calotte cube can be used. The ball bar and the calotte plate need to be measured in different positions in the measurement volume, similar to the use of ball plates for CMMs to determine the spatial distribution of errors. By applying scale correction, i.e. correction of the voxel size as described in [86], sphere distance errors smaller than half the voxel edge length can be achieved. First results indicate, that with corrected CT, single point measurement

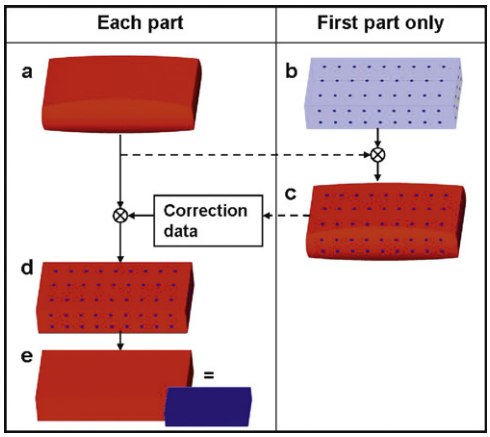

Fig. 23. Auto-correction for CT point clouds: (a) generated CT point cloud, (b) measured reference points with reference sensor, (c) calculated deviations and generated correction data (part specific), (d) corrected CT points, (e) calculated point cloud (blue demonstrates the original workpiece) [28].

uncertainties of the order of the voxel edge length and below become possible (Fig. 23).

Auto-correction methods have been introduced, which directly use the deviations between the CT measurement of the part and reference measurements on the same part, e.g. the real deviations caused by CT, including influences of the material and part geometry are corrected [28]. The correction of CT-point clouds can be done, e.g. by tactile or optical probing, which is capable of measuring points on the part's surface with lower systematic deviation than the CT sensor. The appropriate selection of the regions which are measured with precise sensors is essential for effective correction [29]. The corrected data set is finally stored and can be applied to each CT measurement of parts with the same nominal shape [8,28]. The uncertainty of CT measurement data at interior surfaces (not accessible by tactile or optical probing) can be improved by extrapolation starting on the outer surfaces.

4.5.1. Fusion of CT data

CT data, based on the acquisition of a series of X-ray images and a mathematical reconstruction process, can be classified as an image fusion process but is here presented in the section about coordinate measuring instruments, as CT is developing as one of the most powerful non-destructive evaluation techniques for measurement of dimensional and geometrical quantities. In nearly all industrial CT systems the workpiece is rotated during the acquisition step by step on a rotary table. Together these projections form an image stack which can be fused by mathematical algorithms based on Radon's work of 1917 and implemented by Feldkamp in 1984 [52].

As mentioned in Section 3.4 the quality of CT datasets is affected by the environmental conditions of the measurement. Especially when scanning multi-material specimens with high differences in density, artefacts make a reliable dimensional measurement difficult. To improve measurement results, recent research activities have tried to exploit Dual Energy Computed Tomography (CEXT) [80]. By scanning a specimen using different energies and applying the knowledge about beam attenuation in the material, it is possible to combine information of both reconstructions in order to quantify the different materials of a component. A high energy (HE) macro-focus scan generates nearly artefact-free but blurry, less precise and more noisy data. In contrast, a low-energy (LE) micro-focus measurement generates high precision but artefact affected data (see Fig. 24).

After the pre-processing step to reduce the SNR and artefacts in the data, a registration procedure is applied following a multi-resolution approach. The HE dataset is considered as the fixed image as it is robust to artefacts, whereas the LE dataset is considered as the moving image which is registered to the fixed image. In order to combine the advantages of both measurements,

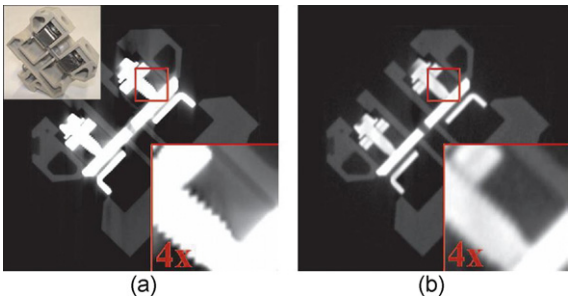

Fig. 24. Cross-section of a micro-CT scan of a terminal block (a) streaking artefacts around the metallic clamps are present. (b) Cross-section of the macro-CT scan. In the area of the screws the disadvantages of the macro-focus CT are revealed and fine structures disappear ©2007IEEE [80].

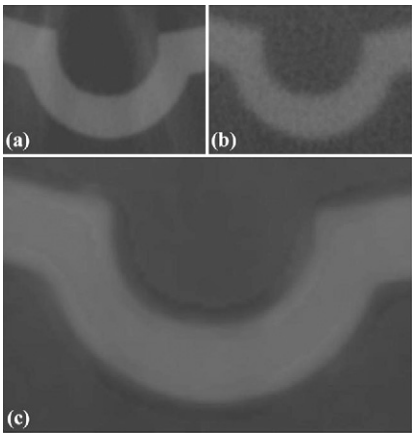

Fig. 25. Axial cross-section through a cutout of a 400-V connector. LE image (a), HE image (b) and fused image (c). After the image fusion the edges are significantly enhanced for surface extraction without keeping artefacts from the LE dataset ©2007IEEE [80].

the main object structure from the HE dataset is fused with the crisp edges of the LE dataset (Fig. 25). An adapted version of weighted arithmetic image fusion at the pixel level is used. It employs a region based encoding of the weights for HE and LE datasets [80].

Further methods for the reduction of artefacts in CT scans are introduced in [166]. The idea of the "dual viewing" process is to capture the species in two different clamping positions within the beam to fuse the areas which are not affected by artefacts. The "multi energy" approach follows the idea of varying the parameters acceleration voltage and energy to fuse the datasets before the reconstruction to achieve the volume data set.

4.5.2. Fusion of tactile, optical and CT data

The present development of CT is determined by the combination of CT with other sensors in multisensor CMMs. Combining X-ray computed tomography (CT) with the design and components of industrial CMMs makes it possible to achieve an accuracy enabling CT being used in industrial coordinate metrology. Neuschaefer-Rube et al. [140] points out that the combination of optical, tactile and CT sensor data does not need to be based on integrating the sensors into multisensor CMMs. Measurements with the objective to achieve holistic geometrical measurement information are carried out on a cast cylinder segment [7,9] and a calotte cube [138].

The outer geometries of the cylinder head segment (Fig. 26a) are measured with a fringe projection system. It exhibits an outer surface (blue) and an inner surface (yellow) decided by the triangles' normal vector. In surface areas which cannot be measured optically, not the blue outer surface, but the subjacent yellow inner surface is visible. Therefore, it can be easily seen in Fig. 26b that inner geometries cannot be measured with optical

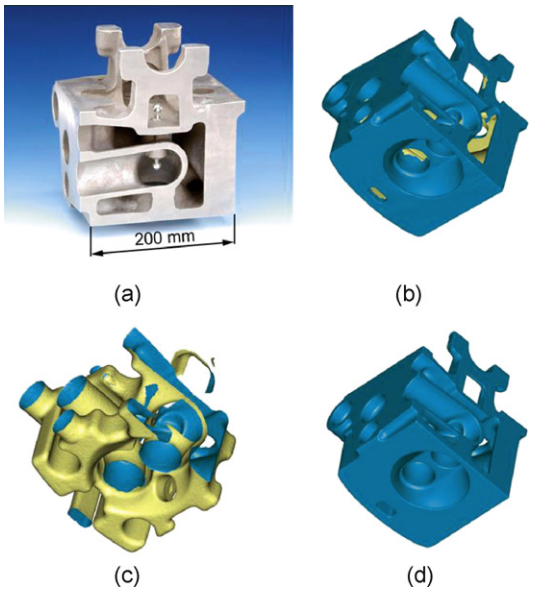

Fig. 26. (a) Segment of a cast cylinder head with reference elements, (b) measurement result with fringe projection, (c) measurement result with CT (outer material surface eliminated), (d) fused data set.

methods. These are captured with a 2D-CT system [161]. After manual segmentation and elimination of the outer material surface, the yellow colored reverse side of the inner interface is visible.

These two data sets were fused to a multisensor data set (see Fig. 26d). The alignment of the two data sets was feature based and carried out on the spherical reference elements partly visible in Fig. 26a. In the regions with overlapping measurement points, the data was smoothed manually. Missing areas of the optical measurement were filled with appropriate regions of the CT measurement. The result was evaluated by comparison with a tactile measurement. The deviations between the fused data set and the tactile data set are, apart from a few exceptions, smaller than ±0.38 mm (approx. voxel size of the CT measurement). The deviations are mainly caused by the suboptimal alignment of the data sets due to the anisotropic point densities between the compared point cloud (tactile measurement) and surface data (optical or CT measurement).

On three faces of the calotte cube (size: 10 mm × 10 mm × 10 mm) a grid of 5 × 5 hemispherical calottes of 0.8 mm diameter is arranged. It was calibrated with a tactile CMM (82 points at each calotte) [139] and measured with an optical sensor based on focus variation (for each face of the calotte 9 × 12 measurement fields were stitched) [39] and a micro-CT system [66] (see Fig. 27) [139].

The three optical measurements at the faces of the cube were fused to one data set. This was carried out feature based with the help of five tactile measured calotte centre positions per face. The same five tactile measured centre positions per face were used to correct the scaling factor of the CT measurement.

Comparison of the optical, tactile and CT measurement was carried out for the calottes. A small scaling deviation between the optical and the tactile measurement (approx. 3 μm) is detected, caused by the stitching of the small areas measured by the optical sensor or by the alignment process. The overall deviations between the tactile and the CT measurement are significantly smaller than the voxel size (18.4 μm). There is again a small systematic residual error of 3–4 μm. Because of the feature-based alignment using five calotte centre positions per face, the systematic effect of misalignment is much smaller than in the measurement of the cast cylinder head segment shown before (see Fig. 28).

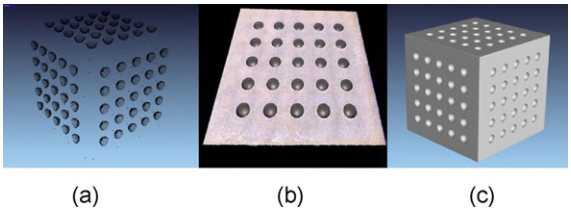

Fig. 27. Measurement results at the calotte cube: (a) tactile, (b) optical (one face), (c) CT.

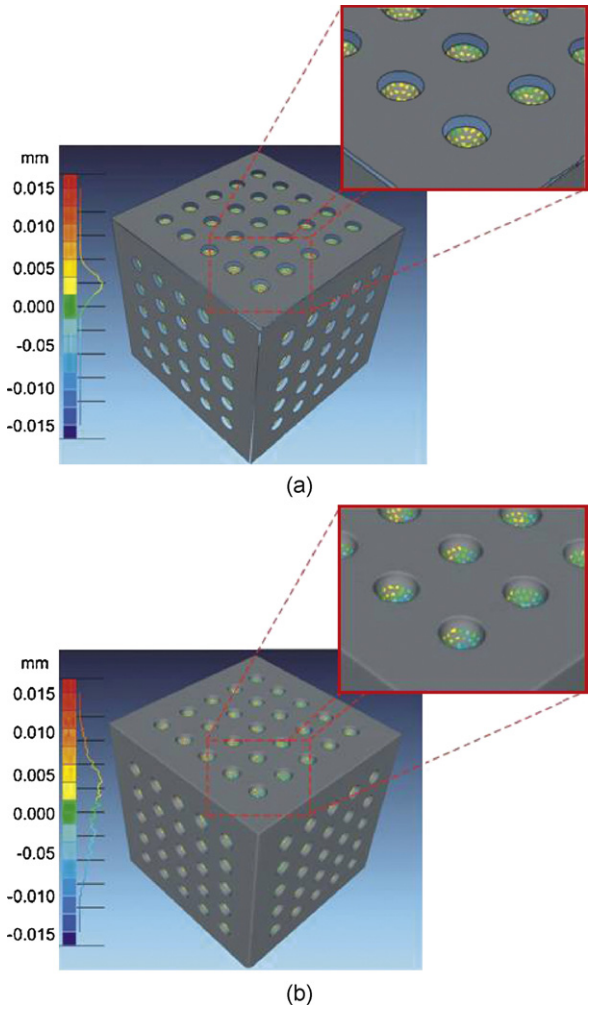

Fig. 28. Results of actual/nominal comparisons at the outer surfaces: (a) tactile measurement (nominal) vs. optical measurement (actual), (b) tactile measurement (nominal) vs. CT measurement (actual).

4.6. Scanning probe microscopy

The family of scanning probe microscopy techniques has revolutionized studies of semiconductors, polymers and nanostructures. Methods to register and fuse AFM data sets as introduced in [50] are applied to increase the accuracy (e.g. due to compensation of the vertical drift [124]) and reliability of topography information. The overall procedure contains the following steps: deconvolution of the tip geometry, registration and data fusion. The registration method is often based on multiresolution techniques, such as the wavelet transformation to detect edge-based features, which can be used for determining the coordinate transformation parameters.

Another method to record a 3D-microtopography is employing scanning electron microscopes (SEMs) in a multi-detector system. To obtain the surface height information it is necessary to use several SEM-images. There exist two different well-known methods to convert 2D images into real 3D surfaces. The stereometric evaluation is only suitable for objects with a sufficient

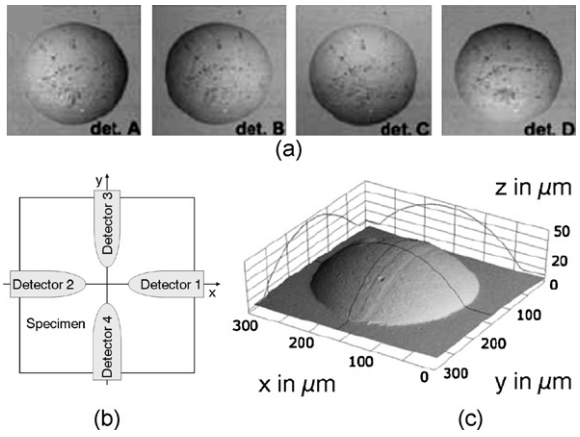

Fig. 29. Scanning electron microscope as a multi-detector system (a) input image set from detector unit (b) hardware configuration (c) reconstructed surface based on [193].

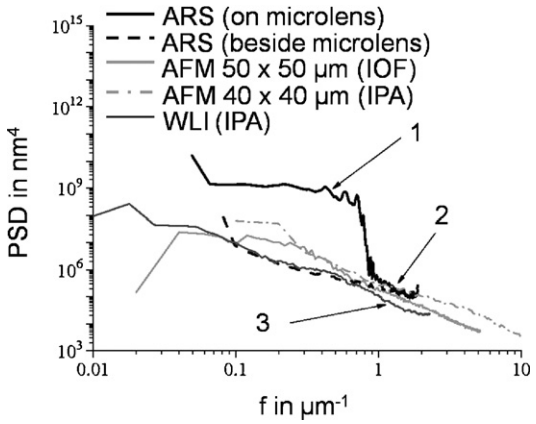

Fig. 30. Roughness spectra: Comparison of PSDs determined by different measurement techniques: 1 influence of beam expansion, 2 range of good agreement, 3 low-pass filter effect through WLI transfer function [154].

amount of distinguishable details and is limited due to the insufficient lateral resolution and measurement area which can be achieved. Professional software solutions are available [3]. An alternative method is the photometric method, which is also applicable to smooth surfaces. This method is also known as 'Shape from Shading', is based on the specific angular distribution of electron emission measured in the multi-detector system. This method was developed by [156] mainly for backscattered electrons. Detector systems based on secondary electrons are presented in [144,193].

Fig. 29 shows the system of four symmetrically placed detectors around the specimen, which produce intensity signals synthesized into four images, which can then be used to reconstruct the surface topography. Images produced by the difference between opposite detector signals demonstrate topographic contrast, whereas their sum creates material composition contrast. The normalized differential signal derived by dividing the two above mentioned signals, leads to the expression for the local surface gradient in the *x*- and *y*-direction. The reconstruction of the surface topography is carried out by areal numerical integration.

Investigations addressing critical factors in SEM 3D stereo microscopy recognized the measurement operation, the instrument calibration and setup and the quality of scanned images as main influencing factors [18,126].

4.7. Monitoring of surface roughness with multisensor systems

One example of multisensor data fusion on the signal level in dimensional metrology is the fusion of the power spectral densities (PSDs) of different data sets into a single PSD of the test specimen. This approach is exemplified on a microlens array in [154]. The test specimen is measured by means of atomic force microscopy, white light interferometry and angle-resolved scattering. Through this, advantages of different sensor principles can be merged to fulfill the requirements concerning measurement scale, resolution, accuracy and time.

The PSD enables a statistical description of the technical surface as a function of the spatial frequency. It can be calculated from any kind of topography data, although its application causes a loss in spatial information. The different PDFs calculated from the measurement data of the sensors are presented in Fig. 30. It is clearly visible, that angle-resolved scattering-PSD provides a continuous changeover between the AFM-PSDs, which are applicable in high frequency domains, and the WLI-PSD, which is adequate for low frequency roughness components. By fusing the PSDs in the confident areas an estimation of the surface PSD was calculated by logarithmical averaging, whereas the single PSD underlie a weighting function. By fusing the power spectral densities of the different data sets over a spatial frequency area of three scales a robust roughness analysis can be completed while

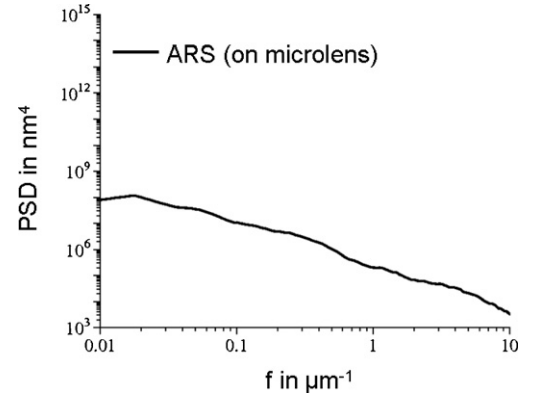

Fig. 31. Estimated PSD of the surface calculated by fusing single PSDs [154].

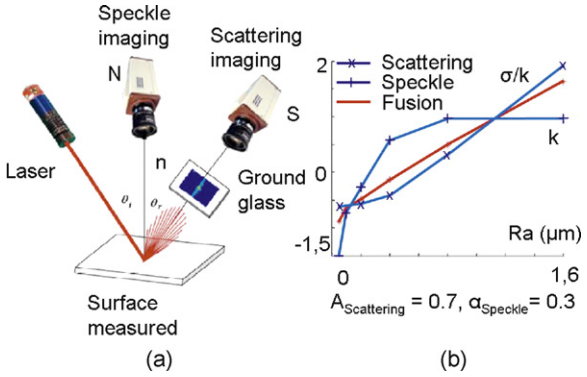

Fig. 32. (a) Hybrid vision system to capture scattering (camera S) and speckle images (camera N); (b) Integration of features (red graph) achieved with speckle and scattering imaging (blue graphs) [189].

simultaneously highlighting typical artefacts of the applied measurement principles (see Fig. 31).

For the online non-contact and high-speed monitoring of surface roughness a hybrid vision system has been developed to capture laser speckle pattern and scattering images with two cameras (see Fig. 32a). Both sensor signals depend on the roughness of the detected surface (see Fig. 32b). The integration of features of both complementary methods improves the linearity of the surface roughness characterization and compensates the low sensitivity of scattering images at low Ra and the low sensitivity of speckle images of high Ra surfaces. Online surface measurement therefore can be obtained with high measurement range [189].

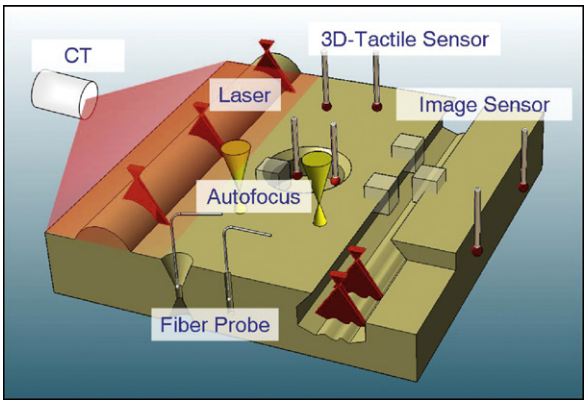

Fig. 33. Cooperative sensor integration in multisensory CMMs. Based on [27].

4.8. Commercially available multisensor CMMs

Multisensor CMMs are characterized by an integrated use of high precision sensors. The application of these cooperative sensor configurations causes several advantages:

1. Different sensors are applied to first achieve an overview of the object. The data from the overview sensor can guide more precise sensors automatically.
2. Inhomogeneous sensors derive information that would not be available from single sensors. The evaluation leads to increased information of object details, an elimination of ambiguities and to a holistic measurement result (see Fig. 33).

The number of commercially available multisensor CMMs is increasing. Manufacturers integrate probing systems developed by themselves or use available probing systems. The Optical Sensor Interface Standard OSIS makes it easier to exchange sensors from different manufacturers and to use different measuring principles [6]. With such multisensor CMMs 2.5D and also 3D measurements can be realized.

Typically 2.5D systems consist of an xy-positioning and measurement stage with various scanning enabled 1D probing systems, similar to many conventional topography and surface roughness measuring systems. They are suited for relatively large flat parts without undercuts, e.g. photolithographically produced, etched or embossed structures and textures with a broad range of height distributions and spatial frequencies. Typically a fixed bridge is used for installing a choice of different sensors such as AFMs, chromatic focus probes, eddy current probes, white light interferometers, conoscopic sensors, confocal point-sensors and others [59]. The relative positions between the sensors fixed to the bridge can be calibrated with the help of appropriate standards, which makes it possible to switch between the sensors. The use of the same coordinate system also facilitates coarse registration of data from different sensors. With 3D measuring sensors it is possible to vastly extend the measuring range by stitching.

3D systems on the other hand are mostly setup according to larger CMMs with modifications especially in the coordinate axes to improve resolution and to reduce measurement uncertainty. A 3D positioning and position measuring system equipped with a 3D probing system is favorable for ensuring maximum flexibility and enabling testing of true 3D geometries with undercuts. Such systems integrate measuring vision systems, different optical and tactile sensors, but also include sensors based on computed tomography or special sensors such as the fiber probe [92,120,136,143,169,204,208]. The method of combining the measurement data of different sensors integrated in such an instrument usually is not published by manufacturers due to commercial reasons. Often, the uncertainty of the different measurement results is not taken into account.

Additionally there are other multisensor examples based on tracked sensors. Either lasers are used to track reflectors or targets on articulated scan arms [5,51,113], or other trackers are applied, i.e. CMMs [129]. The newest developments in this field are hand held scanners [5,35,113,129,132,142,149,158,181].

In addition, white light systems or setups based on photogrammetry (see Section 4.2) belong to the available multisensor coordinate measuring instruments [1,63].

4.9. Available software for registration and fusion of dimensional and geometric data

Every available multisensor CMM contains a multisensor software platform to control the different integrated optical or tactile probing systems and their cooperation [57,92,203,204,121,130]. In addition to these platforms there are several commercial software packages having modules performing multisensor tasks as well as the registration and fusion of the sensor data sets.

Most of them are independent of a specific measuring system [41,93,110,111,131,141,152,176]. Others belong to a CMM manufacturer measuring system, but data can be exchanged via standardized data formats [62,67,114,130,182]. Their commercial application mostly contains the combination of data by portable CMMs and scanners but also other sensor technologies such as computed tomography. The software packages make it possible to create complete models from a set of different single views and usually include methods for the different processing steps: registration, mesh reconstruction and visualization. They further include such aspects as nominal/actual comparison and tolerance analysis.

There are a variety of methods included in the different software packages to align the different data sets such as 3-2-1, RPS (Reference Point System), best fit and 3–10 points align. In reverse engineering software the registration based on standard elements is also implemented. The coarse registration is usually done without knowledge about the measuring position. Special features are the possible implementation into other software packages [176] or functionalities such as the assisted milling based on 3D point clouds [110].

5. Summary and outlook

The demand for information about workpieces in manufacturing started in the 19th century at the beginning of the industrial revolution with two-point-measures. Requirements on improved accuracy have led to the need for geometrical form and position tolerances, which are based mainly on two-dimensional aspects. In recent times there has developed the need for three-dimensional information on features. Currently we see the necessity of availability of holistic information of the whole workpiece in order to predict the performance and quality of a workpiece. The designer must define the whole workpiece as one entity by dimensional and geometrical, macro and micro geometric surface related characteristics with tolerances. For inspection of the workpiece we need suitable instruments being able not only to measure features and their relationship, but we need holistic information of the whole surface and sometimes information regarding the interior structure or defects of the workpiece. Multisensor data acquisition and fusion is the key to solve this task.

Multisensor data fusion is proven to realize measurements with holistic, more accurate and reliable information. Examples of data fusion in metrology have been presented in the field of image fusion, tactile and optical coordinate metrology, coherent and incoherent optical measuring techniques, computed tomography as well as scanning probe microscopy. Despite this wide field of applications, most of the proposed methods are not systematic, but represent rather specific solutions to given problems. Application of fusion methods (i.e. Bayesian approach) as used in robotics and defense are seldom applied in dimensional metrology.

Applications of data fusion in dimensional metrology are of increasing importance in quality control, reverse engineering and

many other industrial fields. However, manufacturing and metrology related requirements result in future challenges:

- *Multiple data models merging and processing*: The fusion methods for the different surfaces captured by different sensor principles must be part of research and development in order to achieve standardized and commonly acknowledged procedures.
- *Multiscale technology*: Products tend to consist of very differently scaled components (Macro > Micro > Nano) with different functionalities in the different scales. The challenge for dimensional metrology lies in making available multiscale measuring devices with suitable concepts for the scale-independent data fusion.
- *Uncertainty of multisensor measurements*: Solutions and standards must be agreed on for fusion of data from different sensor principles of different accuracies.
- *Automation*: The advantages of multisensor systems will be further developed for the automatic conduction of measurements with homogeneous and inhomogeneous probing systems, guiding of these probes and registration and fusion of the data.

The field of multisensor data fusion will continue to be very innovative and interesting in the next decade as it encompasses more and more areas of dimensional metrology.

Acknowledgments

The authors wish to acknowledge the contributions of the following individuals in the preparation of this paper: Markus Bartscher, Daniel B. DeBra*, Leonardo De Chiffre*, R. Freudenberg, Jürgen Goebbels, Uwe Hilpert, Claus P. Keferstein*, Wolfgang Knapp*, Jean-Pierre Kruth*, Graham Peggs*, Enrico Savio*, Michael Schmidt*, Andreas Staude, Jan Thesing. (*CIRP member).

Furthermore we thank Deutsche Forschungsgemeinschaft (German Research Foundation), which gratefully funded some of the underlying research as part of the priority program 1159 "New strategies for measurement and test techniques for production of microsystems and nanostructures" and the collaborative research centre 694 "Integration of Electronic Components into Mobile Systems".

References

[1] Abackerli AJ, Butler BP, Cox MG (1999) Application of Data Fusion Techniques to Thermometry Data, NPL Report CISE 20/99.
[2] Aguilar JJ, Lope M, Torres F, Blesa A (2005) Development of a Stereo Vision System for Non-Contact Railway Concrete Sleepers Measurement Based in Holographic Optical Elements. *Measurement* 38:154–165.
[3] Alicona Imaging GmbH, Producers Documentation, http://www.alicona.com/englisch/products/mex/index.html Accessed 02/2009.
[4] Motavalli S, Suharitdamrong V, Alrashdan A (1998) Design Model Generation for Reverse Engineering Using Multi-Sensors. *IIE Transactions* 30/4:357–366.
[5] Automated Precision Inc., Producers Documentation, http://www.apisensor.-com/ Accessed 10/2008.
[6] Bach C, Boucky O, Keferstein CP, Züst R (2004) Optische Sensoren in der Koordinaten-messtechnik–Software-Schnittstelle standardisiert. *QZ* 49/5:92–95.
[7] Bartscher M, Hilpert U, Goebbels J, Weidemann G, Puder H, Jidav H (2006) Einsatz von Computertomographie in der Reverse-Engineering-Technologie: vollständige Prozesskette am Beispiel eines Zylinderkopfes. *Materialprüfung* 48/6:305–311.
[8] Bartscher M, Hilpert U, Goebbels J, Weidemann G (2007) Enhancement and Proof of Accuracy of Industrial Computed Tomography (CT) Measurements. *Annals of the CIRP* 56/1:495–498.
[9] Bartscher M, Hilpert U (2007) Vergleich von Computertomographie (CT) mit anderer Messtechnik, PTB-report PTB-F-54: 115–124.
[10] Besl PJ, McKay ND (1992) A Method for Registration of 3-D Shapes. *IEEE T-PAMI* 14/2:239–256.
[11] Beyerer J, Puente León F (2005) Bildoptimierung durch kontrolliertes aktives Sehen und Bildfusion. *Automatisierungstechnik* 53/10:493–502.
[12] Beyerer J, Sander J, Werling S (2006) Fusion heterogener Informationsquellen. in Beyerer J, (Ed.) *Informationsfusion in der Mess- und Sensortechnik*. Universitätsverlag Karlsruhe, Karlsruhe, pp. 21–37.
[13] Beyerer J, Sander J, Werling S (2007) Bayes'sche Methodik zur lokalen Fusion heterogener Informationsquellen. *Technisches Messen* 74/3:103–111.
[14] Birch KP, Downs MJ (1993) An Updated Edlen Equation for the Refractive Index of Air. *Metrologia* 30/3:155–162. Art. no. 004.
[15] Boudjemaa R, Forbes AB (2004) Parameter Estimation Methods for Data Fusion, NPL Report CMSC 38/04.
[16] Bradley C, Chan V (2001) A Complementary Sensor Approach to Reverse Engineering. *Journal of manufacturing science and engineering* 123:74–82.
[17] Brassard M, Chahbaz A, Pelletier A, Forsyth DS (2000) Combined NDT Inspection Techniques for Corrosion Detection of Aircraft Structures. *WCNDT, Italy—Proceedings*, . http://www.ndt.net/.
[18] Bariani P, De Chiffre L, Hansen HN, Horsewell A (2005) Investigation on the Traceability of Three Dimensional Scanning Electron Microscope Measurements Based on the Stereo-Pair Technique. *Precision Engineering* 29:219–228.
[19] Carbone V, Carocci M, Savio E, Sansoni G, De Chiffre L (2001) Combination of a Vision System and a Coordinate Measuring Machine for the Reverse Engineering of Freeform Surfaces. *International Journal of Advanced Manufacturing Technology* 17:263–271.
[20] Chan V, Bradley C, Vickers G (2001) A Multi-sensor Approach to Automating Co-ordinate Measuring Machine-Based Reverse Engineering. *Computers in Industry* 44/2:105–115.
[21] Chen F, Brown GM, Song M (2000) Overview of Three-dimensional Shape Measurement Using Optical Methods. *OE* 39/1:10–22.
[22] Chen H, Wang B (2003) Multi-sensor Integrated Automated Inspection System. *Proceedings of SPIE* 5253:528–531.
[23] Chen LC, Lin GC (1997) A Vision-aided Reverse Engineering Approach to Reconstructing Free-form Surfaces. *Robotic and Computer-Integrated Manufacturing* 13(4):323–336.
[24] Chen LC, Lin GC (1997) Reverse engineering of physical models employing a sensor integration between 3D stereo detection and contact digitalisation. *Proceedings of SPIE* 3204:146–155.
[25] Chen LC, Lin GC (1997) An Integrated Reverse Engineering Approach to Reconstructing Free-form Surfaces. *Computer Integrated Manufacturing Systems* 10/1:49–60.
[26] Chou KC, Willsky AS, Benveniste A (1994) Multiscale Recursive Estimation, Data Fusion, and Regularization. *IEEE T-AC* 39/3:464–478.
[27] Christoph R, Neumann HJ (2004) Multisensor Coordinate Metrology. *Verlag Moderne Industrie* .
[28] Christoph R, Rauh W (2008) Measuring Precisely and Traceably Using X-Ray Computed Tomography. *XII International Colloquium on Surfaces—Proceedings*, 346–355.
[29] Christoph R (2008) Measuring precisely and traceably using X-ray computed tomography.CD-ROM *Workshop & Symposium Metrology's Impact on Business, USA—Proceedings*, .
[30] Clark JJ, Yuille AL (1990) *Data Fusion for Sensory Information Processing Systems*. Academic Publishers, Boston/Dordrecht/London.
[31] Collett MA, Cox MG, Esward TJ, Harris PM, Sousa JA (2007) Aggregating Measurement Data Influenced by Common Effects. *Metrologia* 44/5:308–318.
[32] Collett MA, Cox MG, Duta M, Esward TJ, Harris PM, Henry MP (2008) The Application of Self-validation to Wireless Sensor Networks. *Measurement Science & Technology* 19:8. 125201.
[33] Cox MG, Siebert BRL (2006) The Use of Monte-Carlo Method for Evaluating Uncertainty and Expanded Uncertainty. *Metrologia* 43/4:178–188.
[34] Cox MG (2007) The Evaluation of Key Comparison Data: Determining the Largest Consistent Subset. *Metrologia* 44/3:187–200.
[35] Creaform 3D, Producers Documentation, http://www.acticm.com/ Accessed 10/2008.
[36] Cullen JD, Athi N, Al-Jader M, Johnson P, Al-Shamma'a AI, Shaw A, El-Rasheed AMA (2007) Multisensor Fusion for On Line Monitoring of the Quality of Spot Welding in Automotive Industry. *Measurement* 41/4:412–423.
[37] Cuypers W, Van Gestel N, Voet A, Kruth J-P, Mingneau J, Bleys P (2009) Optical Measurement Techniques for Mobile and Large-scale Dimensional Metrology. *Optics and Lasers in Engineering* 47:292–300.
[38] Dad'o S (1996) Limitations of the Metrological Properties of Measurement System Caused by Sensors. *Measurement* 19/1:49–54.
[39] Danzl R, Helmli F (2007) Form Measurement of Engineering Parts Using an Optical Measurement System Based on Focus Variation. *7th EUSPEN International Conference—Proceedings*, 270–273.
[40] Dasarathy BV (1997) Sensor Fusion Potential Exploitation—Innovative Architectures and Illustrative Applications. *Proceedings of IEEE* 85/1:24–38.
[41] DELCAM, PowerINSPECT, Producers Documentation, http://www.powerinspect.com/ Accessed 11/2008.
[42] Deng W, Matuszewski BJ, Shark LK, Smith JP, Cavaccini G (2004) Multimodality NDT image fusion and its mapping on curved 3D CAD surface. *16th World Conference NDT, Canada—Proceedings*, 1023–1030.
[43] Diebel JR, Thrun S, Brünig M (2006) A Bayesian Method for Probable Surface Reconstruction and Decimation. *ACM TOG* 25/1:39–59.
[44] Dietrich B (2007) Maschinenintegrierte Bauteillageerkennung zur Kollisionsprävention mittels skalierbarer Mehrkamerabildverarbeitung, PhD thesis, RWTH Aachen.
[45] Dupuis O, Kaftandjian V, Drake S, Hansen A, Casagrande J-M (2000) Freshex: A Combined System for Ultrasonic and X-Ray Inspection of welds. *15th World Conf. NDT, Italy—Proceedings*, . http://www.ndt.net/ Accessed 08/2009.
[46] Durrant-Whyte HF (1988) Sensor Models and Multisensory Integration. *International Journal of Robotics Research* 7:97–113.
[47] ElMaraghy W, Rolls C (2001) Design by Quality Product Digitization. *Annals of the CIRP* 50/1:93–96.
[48] Esteban J, Starr A, Willetts R, Hannah P, Bryanston-Cross P (2005) A Review of Data Fusion Models and Architectures: Towards Engineering Guidelines. *Neural Computing & Applications* 14/4:273–281.
[49] Estler WT, Edmundson KL, Peggs GN, Parker DH (2002) Large-scale Metrology—An Update. *Annals of the CIRP* 51/2:587–609.
[50] Fan Y, Chen Q, Kumar SA, Baczewski AD, Tram NV, Ayres VM, Udpa L (2006) Registration of Tapping and Contact Mode Atomic Force Microscopy Images. *IEEE-NANO—Proceedings* vol. 1:193–196.

[51] Faro Europe GmbH & Co. KG, Producers Documentation, http://www.faro.com/SelectCountry.aspx Accessed 10/2008.
[52] Feldkamp LA, Davis LC, Kress JW (1984) Practical Cone-beam Algorithm. *JOSA A* 1/6:612–619.
[53] Forbes AB (2000) Fusing Prior Calibration Information in Metrology Data Analysis. in Ciarlini P, (Ed.) *Advanced Mathematical and Computational Tools in Metrology IV*. World Scientific Publishing Company, Singapore , pp. 98–108.
[54] Forbes AB (2001) Efficient Estimators in Data Fusion. in Ciarlini P, (Ed.) *Advanced Mathematical and Computational Tools in Metrology V*. World Scientific Publishing Company, pp. 163–168.
[55] Frankle RS (1993) Practical applications of multimodal NDT data. *Proceedings of SPIE* 1785:184–195.
[56] Francois N (2000) A New Advanced Multitechnique Data Fusion Algorithm for NDT. *15th World Conf. NDT, Italy—Proceedings*, . http://www.ndt.net/ Accessed 08/2009.
[57] Frankowski G, Milsch S, Dietzsch M, Gröger S (2008) Projected Fringe Based Optical 3D Coordinate Measuring Machines—Measuring Accuracy and Applications. *XII International Colloquium on Surfaces—Proceedings*, 278–285.
[58] Fraunhofer-Allianz Vision, http://www.vision.fraunho fer.de/de/4/projekte/272.html Accessed 10/2008.
[59] FRT GmbH, Producers Documentation, http://www.frt-gmbh.com Accessed 10/2008.
[60] Gan Q, Harris CJ (2001) Comparison of Two Measurement Fusion Methods for Kalman-Filter-Based Multisensor Data Fusion. *IEEE T-AES* 37/1:273–280.
[61] Gelfand N, Ikemoto L, Rusinkiewicz S, Levoy M (2003) Geometrically Stable Sampling for the ICP Algorithm. *3DIM 2003*, .
[62] Geomagic Qualify, Producers Documentation http://www.geomagic.com/de/products/qualify/ Accessed 11/2008.
[63] GFMesstechnik GmbH, Producers Documentation, http://www.gfmesstechnik.com/en/index.php Accessed 10/2008.
[64] Gheta I, Heizmann M, Beyerer J (2008) Fusion kombinierter Stereo- und Fokusserien zur 3D-Rekonstruktion. *Technisches Messen* 75:445–454.
[65] Glombitza M (2004) Steigerung der Autonomie fertigungsintegrierter Koordinatenmesssysteme durch flexible Bildverarbeitung, PhD thesis, RWTH Aachen.
[66] Goebbels J, Meinel D, Nötel J, Recknagel Ch (2007) Analysis of morphology and composition with computed tomography exemplified at porous asphalt. *DIR 2007, France—Proceedings*, . http://www.ndt.net/ Accessed 08/2009.
[67] GOM ATOS, Producers Documentation, http://www. gom.com/EN/measuring.systems/atos/system/software/software.html Accessed 11/2008.
[68] Greenleaf AH (1983) Self-Calibrating Surface Measuring Machine. *OE* 22/2:276–280.
[69] Gruen A, Akca D (2005) Least Squares 3D Surface and Curve Matching. *ISPRS Journal of Photogrammetry & Remote Sensing* 59:151–174.
[70] Gros XE (1997) *NDT Data Fusion*. Arnold Publishers, London.
[71] Gühring J (2002) 3D-Erfassung und Objektrekonstruktion mittels Streifenprojektion, PhD thesis, Universität Stuttgart.
[72] Al-Habaibeh A, Shi F, Brown N, Kerr D, Jackson M, Parkin RM (2004) A Novel Approach for Quality Control System Using Sensor Fusion of Infrared and Visual Image Processing for Laser Sealing of Food Containers. *Measurement Science & Technology* 15:1995–2000.
[73] Hagenah H, Schmidt M, Klämpfl F (2008) Planning the Use of High-power Excimer Laser for Psoriasis Treatment. in Mitsuishi M, Ueda K, Kimura F, (Eds.) *Manufacturing Systems and Technologies for the New Frontier—41st CIRP Conference on Manufacturing Systems*. Springer, London, pp. 349–354.
[74] Hall DL, McMullen SAH (2004) *Mathematical Techniques in Multisensor Data Fusion*. Artech House, Norwood.
[75] Hall DL, Llinas J (2001) *Handbook of Multisensor Data Fusion*. CRC Press LLC, Florida.
[76] Hanebeck UD, Briechle K, Harm J (2001) A Tight Bound for the Point Covariance of Two Random Vectors with Unknown but Constraint Cross Correlation. *IEEE Conference on Multisensor Fusion and Integration for Intelligent Systems, Germany—Proceedings*, 85–90.
[77] Hansen HN, Kofod N, De Chiffre L, Wanheim T (2002) Calibration and Industrial Application of Instrument for Surface Mapping based on AFM. *Annals of the CIRP* 51/1:471–474.
[78] Hansen HN, Bariani P, De Chiffre L (2005) Modelling and Measurement Uncertainty Estimation for Integrated AFM-CMM Instrument. *Annals of the CIRP* 54/1:531–534.
[79] Heger T (2005) Erfassung dreidimensionaler Strukturen mit 2D-Bildverarbeitung unter Einsatz gesteuerter Beleuchtung, PhD thesis, Universität Kaiserslautern.
[80] Heinzl Ch, Kastner J, Gröller E (2007) Surface Extraction from Multi-Material Components for Metrology using Dual Energy CT. *IEEE T-VCG* 13/6:1520–1527.
[81] Heizmann M, Puente León F (2003) Imaging and Analysis of Forensic Striation Marks. *OE* 42/12:3423–3432.
[83] Heizmann M, Puente León F (2006) Bildfusion. in Beyerer J, (Ed.) *Informationsfusion in der Mess- und Sensortechnik*. Universitätsverlag Karlsruhe, Karlsruhe, pp. 79–92.
[84] Heizmann M (2006) Image Fusion, Tutorial, MFI 2006, Germany, urn:nbn:de:0011-n-508236.
[85] Heizmann M, Puente Leòn F (2007) Fusion von Bildsignalen. *Technisches Messen* 74/3:130–138.
[86] Hiller J, Kasperl S, Hilpert U, Bartscher M (2007) Koordinatenmessung mit industrieller Röntgen-Computertomographie. *Technisches Messen* 74/11:553–564.
[87] Horbach J (2008) Verfahren zur optischen 3D-Vermessung spiegelnder Oberflächen, PhD thesis, Universität Karlsruhe.
[88] Horn BKP, Brooks MJ, (Eds.) (1989), *Shape from Shading*. MIT Press, Cambridge.
[89] Hughes EB, Wilson A, Peggs GN (2000) Design of a High-accuracy CMM Based on Multi-lateration Techniques. *Annals of the CIRP* 49/1:391–394.
[90] Huicheng Z, Jihong C, Daoshan Y, Ji Z, Buckley S (2000) Datacloud Fusion in Three-dimensional Laser Comparator. *Measurement* 27:93–99.
[91] Hsueh WJ, Antonsson EK (1997) Automatic High-resolution Optoelectronic Photogrammetric 3D Surface Geometry Acquisition System. *Machine Vision and Application* 10:98–113.
[92] Imkamp D, Vizcaino-Hoppe M (2008) *Mehr als die Summe der Sensoren, Optische Sensoren für Multisensor-Koordinatenmessgeräte*. Innovationsforum NORTEC.
[93] Innovmetric, Polyworks, Producers Documentation, http://www.innovmetric.com/Manufacturing/home.aspx Accessed 11/2008.
[94] ISO/IEC Guide 98:1995, Guide to the Expression of Uncertainty in Measurement, (GUM).
[95] ISO/IEC Guide 98-3 Supplement 1:2008-11, Uncertainty of Measurement—Part 3: Guide to the Expression of Uncertainty in Measurement (GUM:1995), Supplement 1: Propagation of Distributions Using a Monte Carlo Method.
[96] Jäger G, Manske E, Hausotte T (2001) Nanopositioning and measuring machine. *2nd EUSPEN International Conference 1*, Turin, 290–293.
[97] Jamshidi J, Owen GW, Mileham AR (2006) A New Data Fusion Method for Scanned Models. *Transactions of the ASME* 6:340–348.
[98] Jamshidi J, Mileham AR, Owen GW (2006) High Accuracy Laser Scanned View Registration Method for Reverse Engineering Using a CMM Generated CAD model. *IDETC/CIE—Proceedings*, 241–248.
[99] Jaynes ET (2003) *Probability Theory: The Logic of Science*. Cambridge University Press.
[100] Kaftandjian V, Zhu YM, Dupuis O, Babot D (2005) The Combined Use of the Evidence Theory and Fussy Logic for Improving Multimodal Nondestructive Testing Systems. *IEEE T-IM* 54/5:1968–1977.
[101] Kalman RE (1960) A New Approach to Linear Filtering and Prediction Problems. *Transactions of the ASME—Journal of Basic Engineering* 82(Series D):35–45.
[102] Kammel S, Horbach J (2005) Topography Reconstruction of Specular Surfaces, Videometrics VIII. *SPIE* 5665:59–66.
[103] Kammel S, Puente León F, Sommer K-D (2007) A Unified Approach to Multisensor Information Fusion and Uncertainty Evaluation. *Workshop & Symposium Metrology's Impact on Business, USA—Proceedings*, . CD-ROM.
[104] Kammel S, Puente León F, Sommer K-D (2008) Modellierung von Vorwissen in der Messtechnik. *14 GMA/ITG-Fachtagung: Sensoren und Messsysteme—Proceedings*, . CD-ROM.
[105] Kapusi D, Machleidt T, Manske E, Franke K-H, Jahn R (2008) White Light Interferometry Utilizing the Large Measuring Volume of a Nanopositioning and Nanomeasuring Machine. *XII International Colloquium on Surfaces—Proceedings*, 210–217.
[106] Keferstein CP, Honegger D, Ritter M (2006) Marktanalyse optischer 1D-, 2D, 3D-Sensoren und optischer KMG. *QZ* 8:40–41.
[107] Kiencke U, Jäkel H (2005) *Signale und Systeme*. Oldenbourg Verlag, München Wien.
[108] Klein LA (2004) *Sensor and Data Fusion—A Tool for Information Assessment and Decision Making*. SPIE Press.
[109] Klämpfl F, Schmidt M, Hagenah H, Görtler A, Wolfsgruber F, Lampalzer R, Kaudewitz P (2006) Irradiation Planning for Automated Treatment of Psoriasis with a High-power Excimer Laser. *Progress in Biomedical Optics and Imaging—Proceedings of SPIE* 6078. Art. no. 60780D.
[110] Knotenpunkt, Pointmaster, Producers Documentation, http://www.knotenpunkt.com/produkte_pointmaster_E.htm Accessed 11/2008.
[111] Kotem, SmartFit 3D, Producers Documentation, http://www.kotem.com/Pages/SmartFit.htm#overview Accessed 11/2008.
[112] Lang P (1999) Multisensorielle Prüfung von Freiformflächen, PhD thesis, University Erlangen-Nürnberg.
[113] Leica Geosystems AG, Producers Documentation, http://www.leica-geosystems.com/ Accessed 10/2008.
[114] Leica Geosystems AG, Producers Documentation, http://www.leica-geosystems.com/corporate/en/ndef/lgs_6515.htm?changelang=true Accessed 11/2008.
[115] Lira I (2002) *Evaluating the Measurement Uncertainty: Fundamentals and Practical Guidance*. Taylor & Francis.
[116] Liu S, Peng K, Zhang X, Zhang H, Huang F (2006) *Proceedings of SPIE* 6357 II. Art. no. 63574H.
[117] Liu X, Li A, Zhao X, Gao P, Tian J, Peng X (2007) Model-based Optical Metrology and Visualization of 3D-complex Objects. *Optoelectronics Letters* 3/2:115–118.
[118] Liu Z, Forsyth DS, Komorowski JP, Hanasaki K, Kirubarajan T (2007) Survey: State of the Art in NDE Data Fusion Techniques. *IEEE T-IM* 56/6:2435–2451.
[119] Luo RC, Yih C-C, Su KL (2002) Multisensor Fusion and Integration, Approaches, Applications, and Future Research Directions. *IEEE Sensors Journal* 2/2:107–119.
[120] Mahr GmbH, Producers Documentation, http://www.mahr.de/ Accessed 10/2008.
[121] MahrVision 3D Reshaper http://www.mahr.de/index.php Accessed 11/2008.
[122] Marinello F, Savio E, Carmignato S, Bariani P, De Chiffre L, Bossard M (2007) Increase of Maximum Detectable Slope with Optical Profilers: Theory and Applicative Examples. *Proceedings of the 7th EUSPEN* 1:333–336.
[123] Marinello F, Bariani P, Pasquini A, De Chiffre L, Bossard M, Picotto GB (2007) Increase of Maximum Detectable Slope with Optical Profilers, Through Controlled Tilting and Image Processing. *Measurement Science & Technology* 18:384–389.
[124] Marinello F, Bariani P, De Chiffre L, Savio E (2007) Fast Technique for AFM Vertical Drift Compensation. *Measurement Science & Technology* 18/3:689–696.
[125] Marinello F, Bariani P, De Chiffre L, Hansen HN (2007) Development and Analysis of a Software Tool for Stitching Three-dimensional Surface

Topography Data Sets. *Measurement Science & Technology* 18/5:1404–1412.
[126] Marinello F, Bariani P, Savio E, Horsewell A, De Chiffre L (2008) Critical Factors in SEM 3D Stereo Microscopy. *Measurement Science & Technology* 19/6:065705.
[127] Matuszewski BJ, Shark LK, Varley MR (2000) Region-based Wavelet Fusion of Ultrasonic, Radiographic and Shearographic Non-destructive Testing Images. *WCNDT, Italy—Proceedings*, . http://www.ndt.net/ Accessed 08/2009.
[128] Mayer JRR, Parker GA (1994) A Portable Instrument for 3D Dynamic Measurements Using Triangulation and Laser Tracking. *IEEE T-RA* 10/3:504–516.
[129] Metris, Producers Documentation, http://us.metris.com Accessed 10/2008.
[130] Metris Camio 6.0, Producers Documentation, http://www.metris.com/products/cmm_software/ Accessed 11/2008.
[131] Metrix, build!IT, Producers Documentation, http://www.mayametrix.com/ Accessed 11/2008.
[132] Metronor AS, Producers Documentation, http://www.metronor.com/ Accessed 10/2008.
[133] Mitchel HB (2007) *Multi-Sensor Data Fusion*. Springer, Heidelberg, ISBN: 978-3-540-71463-7.
[134] Mitchell J, Spence A, Hoang M, Free A (2004) Sensor Fusion of Laser Trackers for Use in Large-scale Precision Metrology. *Proceedings of SPIE* 5263:57–65.
[135] Müller M, Krüger W, Saur G (2006) Robust Image Registration for Fusion. *Information Fusion* .
[136] Mycrona GmbH, Producers Documentation, http://www.mycrona.de/ Accessed 10/2008.
[137] Nashman M, Yoshimi B, Hong HT, Rippey WG, Herman M (1997) A Unique Sensor Fusion System for Coordinate Measuring Machine Tasks. *Proceedings of SPIE International Symposium on Intelligent Systems and Advanced Manufacturing*, 10–97.
[138] Neugebauer M, Hilpert U, Bartscher M, Gerwien N, Kunz St, Neumann F, Goebbels J, Weidemann G (2007) Ein geometrisches Normal zur Prüfung von Röntgen-Mikro-Computertomografiemesssystemen. *Technisches Messen* 74/11:565–571.
[139] Neugebauer M, Hilpert U, Bartscher M, Gerwien N, Krystek M, Schwehn C, Trenk M, Goebbels J, Weidemann G (2008) Untersuchungen zur Messung von Mikrogeometrien mit großen taktilen KMGs und Anwendung bei einem Prüfkörper für Mikro-CT-Messsysteme. *Technisches Messen* 75/3:187–198.
[140] Neuschaefer-Rube U, Bartscher M, Hilpert U (2008) Application of Multisensory Measurements and Sensor Data Fusion in Coordinate Metrology. *Workshop & Symposium Metrology's Impact on Business, USA—Proceedings*, . CD-ROM.
[141] New River Kinematics, Spacial Analyser, Producers Documentation, http://www.kinematics.com/products/sa/index.html Accessed 11/2008.
[142] Northern Digital Inc., Producers Documentation, http://www.ndigital.com/industrial/ Accessed 10/2008.
[143] Optical Gaging Products Inc., Producers Documentation, http://www.ogpnet.com/ Accessed 10/2008.
[144] Paluszyński J, Slówko W (2006) Compensation of the Shadowing Error in Three-Dimensional Imaging with a Multiple Detector Scanning Electron Microscope. *Journal of Microscopy* 224/1:93–96.
[145] Pavese F, Forbes AB (2009) *Data Modeling for Metrology and Testing in Measurement Science*. Birkenhäuser, Boston.
[146] Peggs GN (2003) Virtual Technologies for Advanced Manufacturing and Metrology. *IJCIM* 16/7-8:485–490.
[147] Peggs GN, Maropoulos PG, Hughes EB, Forbes AB, Robson S, Ziebart M, Muralikrishnan. (2009) Recent Developments in Large-scale Dimensional Metrology. *Journal of Engineering Manufacture* 223/6:571–595.
[148] Peng X, Zhang Z, Tiziani HJ (2002) 3-D Imaging and Modeling. Part I. Acquisition and Registration. *Optik* 113/10:448–452.
[149] Polhemus, Producers Documentation, http://www.polhemus.com/ Accessed 10/2008.
[150] Puente León F (2002) Komplementäre Bildfusion zur Inspektion technischer Oberflächen. *Technisches Messen* 69/4:161–168.
[151] Puente León F, Kammel S (2006) Inspection of Specular and Painted Surfaces with Centralized Fusion Techniques. *Measurement* 39:536–546.
[152] Rapidform, XOS-Scan, Producers Documentation, http://www.rapidform.com/Contents/Product/category_id/50 Accessed 11/2008.
[153] Regin J, Neher J, Pannekamp J, Westkämper E, Wiesendanger T, Osten W (2006) Multiskalige Messstrategien für die Systemtechnik. in Beyerer J, (Ed.) *Informationsfusion in der Mess- und Sensortechnik*. Universitätsverlag Karlsruhe, Karlsruhe, pp. 137–143.
[154] Regin J, et al, (2008) Fusion multimodaler Daten am Beispiel eines Mikrolinsenarrays. *Technisches Messen* 75/5:318–326.
[155] Reich C, Ritter R, Thesing J (2000) 3D-shape Measurement of Complex Objects by Combining Photogrammetry and Fringe Projection. *OE* 39/1:224–231.
[156] Reimer L, Böngeler R, Desai V (1987) Shape from Shading Using Multiple Detector Signals in Scanning Electron Microscopy. *Scanning Microscopy* 1/3:963–973.
[157] RevXperts. (2005) Mess- und Digitalisiersystem mit 3D-Navigarionstechnologie. *QZ* 50/7:p76.
[158] RevXperts GmbH, Producers Documentation, http://www.revxperts.com/ Accessed 10/2008.
[159] Ruser H, Puente León F (2006) Methoden der Informationsfusion - Überblick und Taxonomie. in Beyerer J, (Ed.) *Informationsfusion in der Mess- und Sensortechnik*. Universitätsverlag Karlsruhe, Karlsruhe, pp. 1–20.
[160] Ruser H, Puente León F (2007) Informationsfusion–Eine Übersicht. *Technisches Messen* 74/3:93–102.
[161] Saewert HC, Fiedler D, Bartscher M, Wäldele F (2003) Obtaining Dimensional Information by Industrial CT Scanning—Present and Prospective Process Chain. *International Symposium on Computed Tomography and Image Processing, Berlin, DGZfP BB 84-CD*, 163.
[162] Savio E, De Chiffre L, Schmitt R (2007) Metrology of Freeform Shaped Parts. *Annals of the CIRP* 56/2:810–835.
[163] Sawo F, Beutler F, Hanebeck UD (2008) Decentralized Reconstruction of Physical Phenomena based on Covariance Bounds. *IFAC 2008—Proceedings*, .
[164] Schön N, Häusler G (2005) Automatic Coarse Registration of 3D Surfaces. *Vision, Modeling and Visualization—Proceedings*, 171–175.
[165] Schmitt R, Dietrich B, Pollmanns S (2008) Virtual Flight through the Workpiece–3D-Quality Assurance by Means of X-Ray Computer Tomography. *XII International Colloquium on Surfaces—Proceedings*, 336–345.
[166] Schmitt R, Hafner Ph, Pollmanns S (2008) Artefaktreduzierung in tomographischen Aufnahmen mittels Bilddatenfusion.CD-ROM *14 GMA/ITG-Fachtagung: Sensoren und Messsysteme 2008—Proceedings*, .
[167] Schmitt R, Pavim A (2008) Fusion of Micro-metrology Techniques For the Flexible Inspection of MEMS/MOEMS Assembly. *Proceedings of SPIE* 6995. Art. no. 69950I.
[168] Schmitt R, Pfeifer T, Mersmann C, Orth A (2008) A Method for the Automated Positioning and Alignment of Fibre-Reinforced Plastic Structures Based on Machine Vision. *Annals of the CIRP* 57:501–504.
[169] Dr. Heinrich Schneider Messtechnik GmbH, Producers Documentation, www.dr-schneider.de Accessed 10/2008.
[170] Schuster H-F, Förstner W (2003) Segmentierung, Rekonstruktion und Datenfusion bei der Objekterfassung mit Entfernungsdaten - ein Überblick. *2 Oldenburger 3D-Tage, Oldenburg—Proceedings*, .
[171] Schwenke H, Neuschaefer-Rube U, Kunzmann H, Pfeifer T (2002) Optical Methods for Dimensional Metrology in Production Engineering. *Annals of the CIRP* 51/2:685–699.
[172] Schwenke H, Franke M, Hannaford J (2005) Error Mapping of CMMs and Machine Tools by a Single Tracking Interferometer. *Annals of the CIRP* 54/1:475–478.
[173] Seeger S, Laboureux X (2000) *Feature Extraction and Registration—An Overview, Principles of 3D Image Analysis and Synthesis*. Academic Publishers, Boston, Dordrecht, London. 153–166.
[174] Seewig J, et al. (2007) Optisches Messen technischer Oberflächen in der Praxis–Begriffe und Messsysteme, compendium to VDI-Berichte 1996.
[175] Sivia D, Skilling J (2006) *Data Analysis: A Bayesian Tutorial*. Oxford University Press.
[176] 3D Shape, SLIM 3D, Producers Documentation, http://www.3d-shape.com/produkte/slim_e.php Accessed 11/2008.
[177] Shen TS, Huang J, Menq C-H (2000) Multiple-Sensor Integration for Rapid and High-Precision Coordinate Metrology. *IEEE/ASME T-MECH* 5/2:110–121.
[178] Shen T, Huang J, Menq C (2001) Multiple-sensor Planning and Integration for Automatic Coordinate Metrology. *Journal of Computing and Information Science in Engineering* 167–179.
[179] Singh P, Yanyan W, Kaucic R, Jiaqin C, Little F (2007) Multimodal Industrial Inspection and Analysis. *Journal of Computing and Information Science in Engineering* 7/1:102–107.
[180] Sokolov DV, Kasantzev DV, Tyrrell JWG, Hasek T, Danzebrink H-U (2005) Combined Confocal and Scanning Probe Sensor for Nano-Coordinate Metrology. in Wilkening G, Koenders L, (Eds.) *Nanoscale Calibration Standards and Methods*. Wiley–VCH, Weinheim, pp. 131–143.
[181] Steinbichler Optotechnik GmbH, Producers Documentation, http://www.steinbichler.de/en/main/home_2.htm Accessed 10/2008.
[182] Steinbichler COMET plus, Producers Documentation http://www.steinbichler.de/en/main/3d_digitizing.htm Accessed 11/2008.
[183] Stubberud SC, Kramer KA, Geremia JA (2007) Feature Object Extraction: Evidence Accrual for the Level 1 Fusion Classification Problem. *IEEE T-IM* 56/6:2705–2716.
[184] Söll S, Roither B, Moritz H, Ernst H (2007) Three-dimensional Surface Test with "Shape from Shading". *Phonotik International* . (originally published in German in Photonik 4/2006: 74–76).
[185] Sommer K-D, Kuehn O, Puente León F, Siebert BRL (2006) A Bayesian Approach to Information Fusion for Evaluating the Measurement Uncertainty. *IEEE International Conference on Multisensor Fusion and Integration for Intelligent Systems*, 437–441.
[186] Sommer K-D, Siebert BRL (2006) Systematic Approach to the Modelling of Measurements for Uncertainty Evaluation. *Metrologia* 43/4:S200–S210. Art. no. S06.
[187] Sommer K-D (2008) Modelling of Measurements, System Theory and Uncertainty Evaluation. in Pavese F, (Ed.) *Data Modelling for Metrology and Testing in Measurement Science*. Springer.
[188] Thesing J, Behring D, Haig J (2007) Freiformflächenmessung mit photogrammetrischer Streifenprojektion. *VDI-Berichte Band 1996* 231–240.
[189] Tian GY, Lu R-S (2006) Hybrid Vision System for Online Measurement of Surface Roughness. *JOSA A* 23/12:3072–3079.
[190] Tischler, K., Kammel, S., Puente León, F., Sommer, K.-D., A Bayesian Approach to Information Fusion for Sensor Networks, Workshop & Symposium Metrology's Impact on Business, USA—Proceedings: CD-ROM.
[191] Tosello G, Gava A, Hansen HN, Lucchetta G, Marinello F (2009) Characterization and Analysis of Weld Lines on Micro Injection Moulded Parts Using Atomic Force Microscope. *Wear* 266/5-6:534–538.
[192] Tyrrell JWG, Dal Savio C, Krüger-Sehm R, Danzebrink H-U (2004) Development of a Combined Interference Microscope Objective and Scanning Probe Microscope. *Review of Scientific Instruments* 75/4:1120–1126.
[193] Vynnyk T, Seewig J, Reithmeier E (2008) 3D Surface Measurement by Low Voltage Scanning Electron Microscope. *XII International Colloquium on Surfaces—Proceedings*, 102–109.
[194] Wagner Ch (2003) Informationstheoretische Grenzen optischer 3D-Sensoren, PhD thesis, University Erlangen-Nürnberg.

[195] Welch G, Bishop G (2006) *An Introduction to Kalman Filter. TR 95-041*. Department of Computer Science, Univ. of North Carolina at Chapel Hill.
[196] Weckenmann A, Nalbantic K (2003) Precision Measurement of Cutting Tools with two Matched Optical 3D-Sensors. *Annals of the CIRP* 52/1:443–446.
[197] Weckenmann A, Estler T, Peggs G, McMurtry D (2004) Probing Systems in Dimensional Metrology. *Annals of the CIRP* 53/2:657–710.
[198] Weckenmann A, Hoffmann J (2006) Messtechnik für die Mikro-Nano-Integration, Sensoren und Messsysteme 2006. *VDE Tagungsband* 25–29.
[199] Weckenmann A, Hoffmann J, Sommer K-D (2007) Manufacturing Metrology for Micro- and Nanotechnology in Germany. *Workshop & Symposium Metrology's Impact on Business, USA—Proceedings*, . CD-ROM.
[200] Weckenmann A, Kraemer P, Hoffmann J (2007) Manufacturing Metrology—State of the Art and Prospects.CD-ROM *9th International Symposium on Measurement and Quality Control, ISMQC—Proceedings*, .
[201] Weckenmann A, Weickmann J, Hartmann W (2008) Model and simulation of fringe projection measurements as part of an assistance system for multi-component fringe projection sensors. *Proceedings of SPIE* 7102.
[202] Weckenmann A, Shaw L (2009) Function oriented, holistic measurements of cutting tools.CD-ROM *CAT 2009—Proceedings*, .
[203] Wenzel Metromec AG Metrosoft CM, Producers Documentation, http://www.metromec.ch/content/view/8/76/lang,en/ Accessed 11/2008.
[204] Werth Messtechnik GmbH, Producers Documentation www.werthmesstechnik.de Accessed 10/2008.
[205] Westkämper E, Osten W, Regin J, Wiesendanger T (2006) Multiskalige Mess- und Prüfstrategien in der Mikro- und Nanomesstechnik. *VDI-Berichte Band 1950* 141–150.
[206] Xin B, Heizmann M, Kammel S, Stiller C (2004) Bildfolgenauswertung zur Inspektion geschliffener Oberflächen. *Technisches Messen* 71/4:218–226.
[207] Zacher M (2004) Integration eines optischen 3D-Sensors in ein Koordinatenmessgerät für die Digitalisierung komplexer Oberflächen, PhD thesis, RWTH Aachen.
[208] Carl Zeiss Industrielle Messtechnik GmbH, Producers Documentation, www.zeiss.de Accessed 10/2008.
[209] Zhao H, Anwer N, Bourdet P (2009) A PLM-Based Multiple Sensor Integration Measurement System for Geometry Processing.CD-ROM *CAT 2009—Proceedings*, .
[210] Zimmermann J, Regin J, Lyda W, Wiesendanger T, Sawodny O, Westkämper E, Osten W (2008) Definition and Design of an Automated Multiscale Measuring System. *EUSPEN 2008—Proceedings* vol. II:425–430.
[211] Zitová B, Flusser J (2003) Image Registration Methods: A Survey. *Image and Vision Computing* 21:977–1000.